# Towards a method for detecting the potential genotoxicity of nanomaterials

NANOGENOTOX

Deliverable 4.3: Crystallite size, mineralogical and chemical purity of NANOGENOTOX nanomaterials

Key intrinsic physicochemical characteristics of NANOGENOTOX nanomaterials

October
2012

Co-funded by
the Health Programme
of the European Union

NANOGENOTOX        **Grant Agreement n° 2009 21 01**

NANOGENOTOX

Grant Agreement n° 2009 21 01

WP 4: Physicochemical Characterization of Manufactured Nanomaterials (MNs) and Exposure Media (EMs)

Deliverable 4.3: Crystallite size, mineralogical and chemical purity of NANOGENOTOX nanomaterials

–

Key intrinsic physicochemical characteristics of NANOGENOTOX nanomaterials

Deliverable leader: NRCWE

Keld Alstrup Jensen

The National Research Centre for the Working Environment (NRCWE),

Lersø Parkallé 105, DK-2100 Copenhagen, DENMARK

National Research Centre
for the Working Environment

| Workflow | |
|---|---|
| **Author(s)** | **Reviewer(s)** |
| Renie Birkedal (NRCWE) | WP Leader: Keld Alstrup Jensen (NRCWE) |
| Boris Shivachev, Louiza Dimova,Ognyan Petrov, Rosica Nikolova (IMC-BAS) | Coordinator: Nathalie Thieriet (ANSES) |
| Jan Mast, Pieter-Jan De Temmerman, Nadia Waegeneers, Lotte Delfosse, Fréderic Van Steen, Jean Christophe Pizzolon and Ludwig De Temmerman (CODA-CERVA), | |
| Vivi Kofoed-Sørensen, Per A Clausen (NRCWE) | |
| Ashley Parks, P. Lee Ferguson (Duke University) | |
| Charles Motzkus (LNE) | |
| Keld Alstrup Jensen (NRCWE) | |

Document status:  v.1      first draft                    Creation date:        9/01/2012
                  v.1.1    second draft                   date:                23/04/2012
                  v.1.2    third draft                    date:                 4/10/2012
                  v.1.2    final revision and review by KAJ    date:            5/10/2012
                  v.1.3    comment from NGTX coordination team   date          11/02/2013
                  v.1.4    revision and review by authors    date             24/03/2013

| Confidentiality level of the deliverable | | |
|---|---|---|
| **PU** | Public | PU |
| **CO** | Confidential, only for members of the consortium (including the Commission Services) | |

# 1 Introduction

This report presents the final results and description of the standard operation procedures (SOPs) for characterization of manufactured nanomaterials regarding their crystalline and chemical composition, phase and chemical purity, as well as quantification of organic compounds, which may be present as either chemical stabilizers, dispersants or surface modifications. In addition to general data presentation, the report also contains an evaluation of the vial to vial and intra-vial variability in X-ray diffraction and thermogravimetric analysis. A special effort was set on comparisons different size-determinations of crystallite size by X-ray diffraction and the bulk inorganic composition of CNT.

The results have been generated during the first two years of the Joint Actions project, NANOGENOTOX, which is funded by the EAHC (Executive Agency for Health and Consumers). Temporary results and SOPs have previously been reported in Guiot et al (2010) and Jensen et al., (2010). This report fulfils the part of deliverable 4 of the project, which concerns the mineralogical and chemical composition of the samples studied in NANOGENOTOX. The analyses were made by NRCWE (Denmark), IMC-BAS (Bulgaria), and CODA-CERVA (Belgium). Contributing data were delivered by LNE (France) and Duke University (USA). The complete deliverable 4 is submitted in 6 topical reports and a final summary report.

The complete list of final report series on physico-chemical characterization are listed hereafter:

> D4.1: Summary report on primary physiochemical properties of manufactured nanomaterials used in NANOGENOTOX
>
> D4.2: Transmission electron characterization of NANOGENOTOX nanomaterials
>
> D4.3: Crystallite size, mineralogical and chemical purity of NANOGENOTOX nanomaterials
>
> D4.4: Determination of specific surface area of NANOGENOTOX nanomaterials
>
> D4.5: Surface charge, hydrodynamic size and size distributions by zetametry, dynamic light scattering (DLS) and small-angle X-ray scattering (SAXS) in optimum aqueous suspensions for titanium and silicon dioxide
>
> D4.6: Dustiness of NANOGENOTOX nanomaterials using the NRCWE small rotating drum and the INRS Vortex shaker
>
> D4.7: Hydrochemical reactivity, solubility, and biodurability of NANOGENOTOX nanomaterials.

Note that the current listed physico-chemical data are considered the final data. The detailed SOPs used to achieve the data are shown in the Appendix of this report.

## 2 Nanomaterials and information given by suppliers

The tested NANOGENOTOX materials include 6 titania-based ($TiO_2$) products, 5 synthetic amorphous silica (SAS) products and 6 multi-walled carbon nanotubes (MWCNT) (Table 2.1). Silica is described as SAS or $SiO_2$, despite amorphous silica usually is oxygen deficient and should be denoted $SiO_x$.

*Table 2-1 Nanomaterials included in the NANOGENOTOX project and information given by suppliers.*

| Code | Special notes | Phase | application | Purity wt% | Particle size | BET ($m^2/g$) | impurity / coating |
|------|---------------|-------|-------------|-----------|---------------|----------------|---------------------|
| NM-100 | Dry-milled | Anatase | paper loadings, rubber, cosmetics, adhesives, low cost interior paints | 98.5 | 200-220 nm | - | - |
| NM-101 | | Anatase | semiconductor catalyst for use in photocatalytic processes | 91(99)* | < 10 nm | >250 | 9%* |
| NM-102 | | Anatase | photocatalytic | 95 | - | 90 | - |
| NM-103 | hydrophobic | Rutile | cosmetics (sun care, colour), pharma, food | 89 | 20 nm | 60 | Al2O3 6%,  silicone - Dimethicone 2% |
| NM-104 | hydrophilic | Rutile | | 90 | 20 nm | 60 | Al2O3 6% - Dimethicone 2% |
| NM-105 | | rutile/anatase | catalysis, heat stabilizer | - | 21 nm | 50+/-15 | - |
| NM-200 | precipitated | PR-A-02 | food, processing | - | 15 um | 220 | 10 SiO2 1 H2O, 2% soluble salts |
| NM-201 | precipitated | PR-B-01 | reinforcement, mechanical and optical properties and process | - | - | 160 | 10 SiO2 1 H2O, 1,5% soluble salts |
| NM-202 | thermal | PY-AB-03 | inks, adhesives, cosmetics, reinforcement, powder process, food, pharmaceuticals | >99,8 | - | 170-230 | - |
| NM-203 | thermal | PY-A-04 | food, cosmetics pharma, reinforcement | - | 12 nm | 200+/-25 | hydrates? |
| NM-204 | Precipitated | | food | - | - | 140 | - |

* calcination causes loss of 9 wt% and the residual is 99% pure

6

**www.nanogenotox.eu**

Co-funded by
the Health Programme
of the European Union

| Code | Special notes | Phase | application | Purity wt% | CNT tube length | BET (m$^2$/g) | impurity / coating |
|---|---|---|---|---|---|---|---|
| NM-400 | CCVD | MWCNT | structural composite and energy applications | - | ~1.5 um long | 250-300 | 10 wt% oxides/coated with pyrogenic carbon |
| NM-401 | CCVD | MWCNT | structural composite and energy applications | - | 5-15 um long | 40-300 | ~2% amorph. carbon |
| NM-402 | CCVD | MWCNT | structural composite and energy applications | - | 0.1-10 um long | - | <10 wt% |
| NM-403 | CCVD | MWCNT | structural composite and energy applications | - | 1->10 µm long | - | - |
| NRCWE-006 | CVD | MWCNT | energy / Li-ion battery | >99.5 | segments; 3-5 um long | 24-28 | |
| NRCWE-007 | CCVD | MWCNT | structural composites etc. | - | 8-15 nm OD; 10-50 um long | 233 | ca. 3.2 wt% C impurties/ < 1.5wt% ash (Al, Cl, S) |

**www.nanogenotox.eu**

Co-funded by
the Health Programme
of the European Union

# 3 X-Ray Diffraction (XRD)

X-Ray Diffraction (XRD) analysis is based on the principle that crystalline materials diffract X-rays in a characteristic pattern, which is unique for each material. XRD can therefore be used to identify different polymorphs, such as typical $TiO_2$ polymorphs rutile, brookite and anatase. The width of the reflections can also give information about the size of the diffracting crystals (not necessarily the same as the particle size).

XRD can be measured in different setups and different wavelengths are possible, but for standard measurements this is less important, as long as it is taken into account. Most databases are based on irradiation using Cu X-rays. The step length (if using Cu) is recommended to be 0.15. (Hill, 1986)

**All data presented in this report were recorded in reflection mode using Cu radiation**, which is usually chosen for fast phase identification. Reflection mode analysis has the advantage that very small samples can be used (though more material is recommended) and the scatter is usually low until high values of $2\theta$, so unit cells can be determined with high accuracy. Internal standards are used to control for differences between instruments.

## 3.1 Instruments

### 3.1.1 Instrument used by NRCWE

The data from NRCWE were measured at room temperature (25°C) on a Bruker D8 Advanced diffractometer in reflection mode with Bragg-Brentano geometry. The analysis were made using $Cu_{K\alpha 1}$ X-rays (1.5406 Å) generated using a sealed Cu X-ray tube run at 40 kV and 40 mA. The x-ray beam was filtered for $Cu_{K\alpha 2}$ and focused using a primary beam Ge monochromator and fixed divergence slit 0.2°. The analyses were made in the stepping mode stepping 0.02 degree $2\theta$ per second and data were collected using a linear PSD detector (Lynx-eye) with opening angle 3.3°.

### 3.1.2 Instrument used by IMC-BAS

The data from IMC-BAS were measured at room temperature (21°C) using a Bruker D2 Phaser diffractometer in reflection mode with $\theta$-$\theta$ geometry. Cu X-rays were generated by a sealed Cu X-ray tube run at 30 kV and 10 mA and focused using a Ni filter and a fixed 0.2° divergence slit. Data generated with a step size of 0.02 degree $2\theta$ and with a step time of 10 s and collected scintillation detector with opening angle 0.2°. Since the instrument does not use a monochromator, the raw data contains reflections from both $K_{\alpha 1}$ and $K_{\alpha 2}$ rays. For data comparison, the $K_{\alpha 2}$ contribution was therefore stripped from the data using the EVA software (Bruker).

### 3.1.1 Instrument used by LNE

The data from LNE were measured on X'pert Pro MPD diffractometer. The X'pert Pro MPD diffractometer has a goniometer configuration $\theta$ - $\theta$, which allows characterization of powders at high diffraction angles. LNE determined the association of Nickel filter, masks, slot and anti-scatter

since these conditions leads to better results resolution / intensity spectrum exclusively for these analysis on specifics powders. The diffractograms were obtained with a scan on range of 2θ from 3 to 140°. The stepping of the goniometer was fixed for these tests to 0.03° for an acquisition time of 30 s. The chamber temperature was 25°C. Analyses were performed with Anode X-Ray tube Cu at 50kV and 35mA.

## 3.2 Instrument contribution

Each instrument has a unique contribution to the X-ray diffraction profile, which should be documented for the detailed data comparisons between NRCWE and IMC-BAS using e.g., a large crystallite standard. For the analysis, IMC-BAS used quartz ($SiO_2$) (NIST SRM1878, median particle size of 1.4 μm after grinding) and NRCWE used a $CeO_2$ (NIST SRM674a) standard. To assess the contribution from the two instruments, the full width at half maximum, FWHM, was measured on the standards and plotted as a radian angle. It is seen that the contribution from the instrument is greater and with some variability for the instrument at IMC-BAS than the instrument used by NRCWE. The listed theoretical functions give the best fit for the measured values and are only valid within the measured range. There will be no minima or maxima for the instrument contribution and therefore the functions have no physical meaning. They do, however, give the best estimate within the measured range and has therefore been chosen prior to a function with more physical meaning. As LNE participated as a contributing partner early in the project, they were not involved in the later detailed instrument and interlaboratory comparison study.
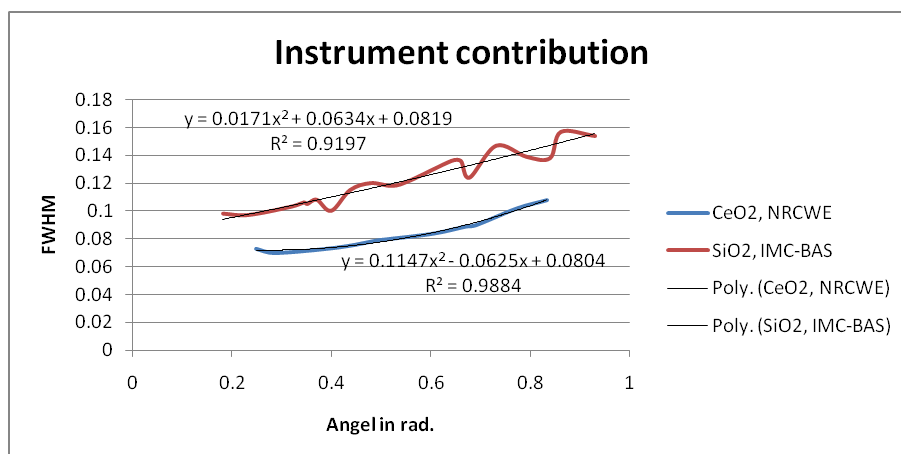


*Figure 3-1. Graph of instrument contribution to the width of the reflections for data collected by NRCWE and IMC-BAS.*

Table 3-1 shows the theoretical contribution from the instruments at IMC-BAS and the instrument used by NRCWE. The instrument contribution is found as the FWHM of the reflections in the dataset of the standards. 2θ is expressed in radians. For each instrument the best fit for FWHM (standard) as a function of 2θ (in radians) is found. From the equations the difference between the two instruments is calculated for four specific points.

It is evident that the instrumental contribution matters most when the reflections are narrow, i.e. for large crystals. The effect of this is clearly seen when e.g. comparing the first reflection for the samples containing anatase, NM101, NM102, NM105 and NM100 (Figure 3-2). Here both a visual and

9

a quantitative relative "left switch" is observed for data measured by ICM-BAS as compared to data from NRCWE. The listed FWHM values are found by calculations using the Bruker EVA software.

*Table 3-1. List of reflection widths for the instrument at IMC-BAS and the one used by NRCWE.*

| 2θ | rad | IMC-BAS | NRCWE | difference | Comment |
|---|---|---|---|---|---|
| 25.31 | 0.220871 | 0.096737 | 0.072191 | 0.0245464 | Anatase, highest reflection |
| 27.434 | 0.239407 | 0.098058 | 0.072011 | 0.0260473 | Rutile, highest reflection |
| 50 | 0.436332 | 0.112819 | 0.074966 | 0.0378526 | |
| 75 | 0.654498 | 0.13072 | 0.088628 | 0.0420926 | |
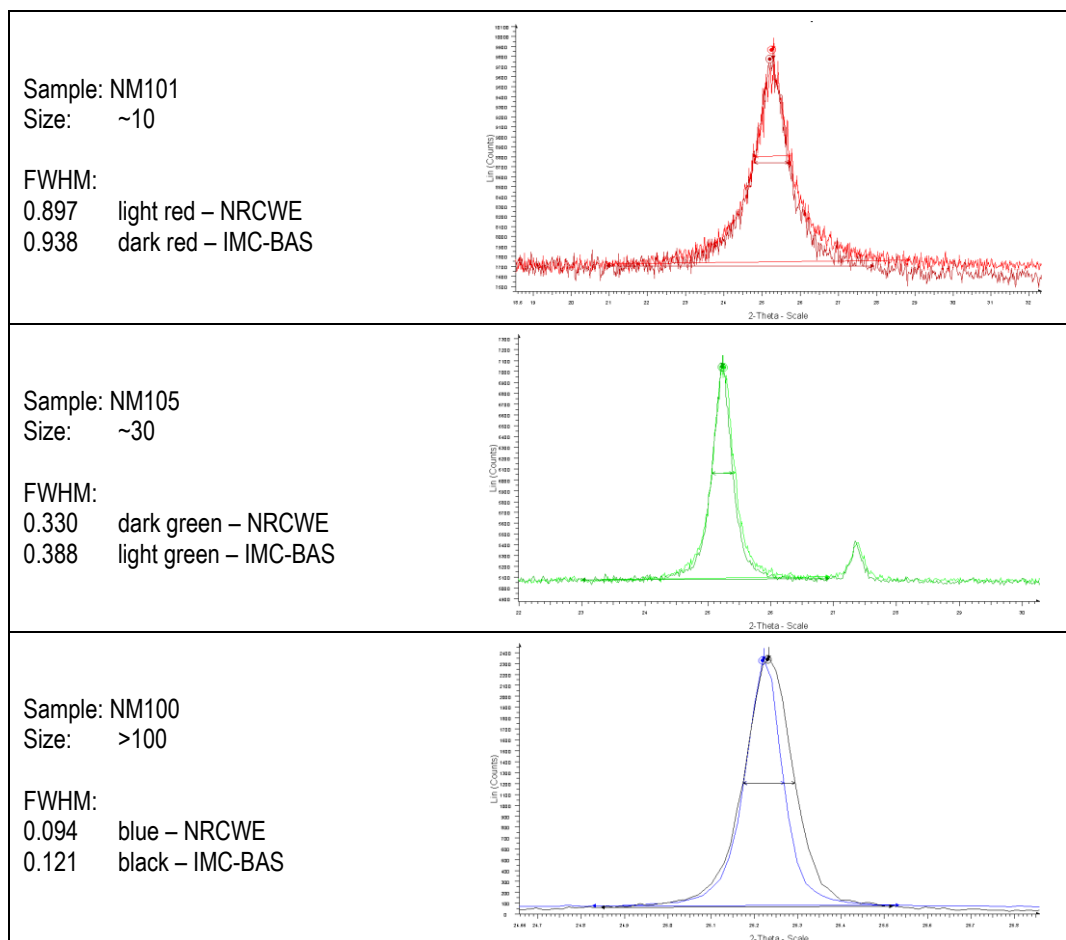


*Figure 3-2. The first reflection of anatase for samples with three different particle sizes. Note that the larger the particles are, the narrower the reflections are, and the more the instrument contribution matters. Direct visual comparison was enabled by scaling the NRCWE diffractograms to the height of the IMC-BAS data shift the position so reflections start at the same angle.*

## 3.3 Samples

As listed in Table 2.1, three different types of materials (TiO2, SAS, and MWCNT) have been studied in NANOGENOTOX. Sample vial numbers have been recorded to ensure that all analyses was not made on consecutive sample vials. All analyzed vials are listed in Table 3-2.

The $TiO_2$ samples are crystalline and contain Anatase, Rutile or a mixture of both. XRD can be used to determine which polymorph is in the sample. If the crystals are smaller than 100 nm, XRD can be used to calculate the size of the crystals.

The SAS are principally amorphous and XRD can therefore not give information on the silica-phase unless it has crystallized or it contains other crystalline (undesired) impurities.

MWCNT can not be analyzed well by the use of the instruments used in this study. There is only one strong and wide reflection around $2\theta = 25.7$ (for Cu radiation). This reflection is most likely related to the distance between the walls in the MWCNT. However, catalyst impurities may be detected before or at least after removal of the carbon in the sample, e.g. by burning in thermogravimetric analysis.

*Table 3-2 List of vials measured with XRD by IMC-BAS, LNE and NRCWE for testing of crystallite sizes, impurities, repeatability and homogeneity in connection with the NANOGENOTOX project.*

| Material | Sample Name | Compound | Vial number(s) | Measured by | | |
|---|---|---|---|---|---|---|
| | | | | NRCWE | IMC-BAS | LNE |
| $TiO_2$ | NM100 | Anatase | 0006 | X | | |
| | | | 0007 | X | | |
| | | | 0016 | | | X |
| | | | 0079 | | X | |
| | | | 0081 | | X | |
| | | | 0083 | | X | |
| | | | 0211+213+214[€] | X (pooled) | | |
| | | | 0406 | X | | |
| | | | 0408 | X | | |
| $TiO_2$ | NM101 | Anatase | 0239 | X | | |
| | | | 0415 | X | | |
| | | | 0510 | X | | |
| | | | 0729 | X | | |
| | | | 1266 | | X | |
| | | | 1268 | | X | |
| | | | 1270 | | X | |
| $TiO_2$ | NM102 | Anatase | 0012 | | | X |
| | | | 0092 | | X | |
| | | | 0094 | | X | |
| | | | 0095 | | X | |
| | | | 0121 | X | | |
| | | | 0477 | X | | |
| | | | 1000 | X | | |

| Material | Sample Name | Compound | Vial number(s) | Measured by | | |
|---|---|---|---|---|---|---|
| | | | | NRCWE | IMC-BAS | LNE |
| TiO$_2$ | NM103 | Rutile | 0223 | X | | |
| | | | 0280 | | | X |
| | | | 0281 | | | X |
| | | | 0547 | | | X |
| | | | 0615 | | X | |
| | | | 0617 | | X | |
| | | | 0618 | | X | |
| | | | 2097 | X | | |
| TiO$_2$ | NM104 | Rutile | 0228 | X | | |
| | | | 0287 | | | X |
| | | | 0289 | | | X |
| | | | 0416 | X | | |
| | | | 0440 | X | | |
| | | | 0451 | | | X |
| | | | 0529 | | X | |
| | | | 0530 | | X | |
| | | | 0533 | | X | |
| TiO$_2$ | NM105 | Anatase Rutile | 0051 | X | | |
| | | | 0058 | X | | |
| | | | 0078 | X | | |
| | | | 0431 | | | X |
| | | | 0438 | | | X |
| | | | 2135 | X | | |
| | | | 2167 | | | X |
| | | | 2242 | | X | |
| | | | 2244 | | X | |
| | | | 2247 | | X | |
| SiO$_2$ | NM200 | | 0072 | X | | |
| | | | 0080 | | | X |
| | | | 0156 | | X | |
| | | | 0157 | | X | |
| | | | 0441 | X | | |
| SiO$_2$ | NM201 | | 0022 | X | | |
| | | | 0027 | | | |
| | | | 0100 | | X | |
| | | | 0102 | | X | |
| | | | 0444 | X | | |
| SiO$_2$ | NM202 | | 0027 | X | | |
| | | | 0039 | | | X |
| | | | 0104 | | X | |
| | | | 0108 | | X | |
| | | | 0486 | X | | |

12

| Material | Sample Name | Compound | Vial number(s) | Measured by | | |
|---|---|---|---|---|---|---|
| | | | | NRCWE | IMC-BAS | LNE |
| SiO$_2$ | NM203 | | 0152 | X | | |
| | | | 0200 | | | X |
| | | | 0280 | | X | |
| | | | 0282 | | X | |
| | | | 0363 | X | | |
| SiO$_2$ | NM204 | | 0006 | X | | |
| | | | 0034 | | | X |
| | | | 0098 | | X | |
| | | | 0102 | | X | |
| MWCNT | NM400 | | 0447 | | X | |
| | | | 0450 | | X | |
| MWCNT | NM401 | | 0103 | | X | |
| | | | 0106 | | X | |
| MWCNT | NM402 | | 0462 | | X | |
| MWCNT | NM402 | | 0467 | | X | |
| MWCNT | NM403 | | 01067 | | X | |
| | | | 01071 | | X | |
| MWCNT | NRCWE-006 | | No vial number | | X | |
| MWCNT | NRCWE-007 | | No vial number | | | |

## *3.4  Sampling mounting*

### 3.4.1  Mounting samples at NRCWE

Figure 3-3 shows the sample holders used by NRCWE.

All TiO$_2$ samples were measured in a standard sample holder, 2.5 cm in diameter and approximately 1 mm deep, made of PMMA. The samples were filled in the sample holders and a glass plate was used to press the material into the holder and level the sample surface with the sample holder.

The Synthetic Amorphous Silica (SAS) samples were very difficult to mount in a standard sample holder. The sample seem to "jump out" of the sample holders with only the slightest disturbance e.g. when using the glass plate to press the samples into the holders. Instead they were mounted with vacuum grease in a single crystal Si low background sample holder. Measurements of empty sample holder with vacuum grease only showed an amorphous signal in the XRD spectrum.

The powder samples were mounted by smearing as little vacuum grease as possible on the Si sample holder. Then the powder sample was topped on the sample holder and vacuum grease. The most important disadvantage of this procedure is a small shift of the zero point, as the sample is not entirely in the correct position.

13

No MWCNT were measured by NRCWE.



*Figure 3-3 showing the two types of sample holders used by NRCWE. To the left is the Si low background sample holder with a Synthetic Amorphous Silica sample. To the right is a standard sample holder with a TiO$_2$ sample. At the top is a Danish "2 krone". (25 mm in diameter)*

### 3.4.2 Mounting samples at IMC-BAS

All TiO$_2$, Carbon-Nanotubes and Synthetic Amorphous Silica samples were measured in a standard plastic sample holder, 2.5 cm in diameter and 1 mm deep. The samples were filled in the sample holders and a glass plate was used to press the material into the holder, to ensure a flat sample with the correct height, the same as height of the sample holder.

The Synthetic Amorphous Silica samples were very difficult to mount (as observed by NRCWE) however, after several trials the material managed to fill and hold in the sample holder.

### 3.4.3 Mounting samples at LNE

The samples were stored at 20°C. For analysis, nano-TiO$_2$ powders were prepared and placed in sample holders for Spinner. During the diffraction analysis, the samples were rotated in order to increase the diffraction phenomena on all the crystals in the sample. Thus, the value of the ratio resolution/intensity was high and allowed the treatment of diffractograms. The analyses were performed for two samples (two bottles) of each reference (NM).

## 3.5  Calculation methods

Many programs are available for calculation on XRD data can directly calculate the crystal size. It can be quite difficult to find their actual way of calculation, but they are more or less based on the same principles of the Scherrer Equation, stating that the wider the reflections the smaller the crystals (see below and in appendix).

At IMC-BAS the diffractogram were processed using three types of software:

1. Fullprof, freely available at http://www.ill.eu/sites/fullprof/;
2. TOPAS® application with the Bruker AXS®;
3. Winfit, a freeware that does not include Rietveld refinement, instead it uses a single or multi-peak fitting procedure and the Scherrer equation (4.1)

14

NRCWE have chosen 2 types of software for calculations of the XRD data:

1. The Scherrer equation was used on data from "fityk", a program only calculating the best fit for the reflections.
2. TOPAS, reporting both the size based on IB (integral breath) and FWHM (full width at half maximum).

LNE performed their calculations according to the "Reference Intensity Ratio (RIR)".

The principle of this method is based on the determination of the intensity ratios between main peaks in relation to that of corundum in 50/50 mixture. RIR is recorded for rutile and anatase in the ICDD database (the International Centre for Diffraction Data). This method can be considered quantitative if there are only two main phases in the $TiO_2$ powder: e.g., anatase and rutile. The number of samples for analysis for each concentration must be at least 2 to estimate the repeatability of the measurement.

## 3.5.1  XRD sizing limitations

As any method, sizing of crystallites by XRD has limitations. Most importantly, the method has both upper and lower limits, where the lower limit is very much material dependent. As discussed, large crystals have narrow reflections, and as rule of thumb, sizes cannot be calculated for crystals larger than 100 nm.  As an example, using the first reflection from Anatase as starting point, and using the Scherrer Equation backwards, this gives the expected additional broadening of 0.014. Compared to the contribution from the instrument 0.072 from NRCWE and 0.097 from IMC-BAS, it is seen that the instrument contribution contributes most to the resulting peak.

Another issue when calculating the crystal size from X-Ray diffraction is how accurate the results really are. In this report we have chosen to list the results as they are calculated by the different methods / programs. At NRCWE it has been decided to round the sizes to whole numbers and list those as results; however for the comparison the numbers have been listed with one decimal.

The real and important question is however; how accurate are the calculations? We know that the larger the crystals get, the more the instrument contribution matters. However for very small crystals it is difficult to find the background and thereby the height of the reflection, so in this case it is also difficult to find the right FWHM, and calculate the right size. We assume that the results are more uncertain than we have listed. Our estimate is that the uncertainty probably is on the order of ±5 nm for all the samples.

Co-funded by
the Health Programme
of the European Union

### 3.5.2 Reported size and standard deviation

Due to different methods, strategies and traditions, data are reported from the three contributors in slightly different ways explained below:

IMC-BAS

The sizes reported by IMC-BAS are based on averages of n analysis or the result of single Rietveld analysis with the calculated uncertainty.

NRCWE

As part of the analysis, NRCWE invested vial homogeneity in the samples why the same vials often have been measured several times. For these measurements each dataset has been used for calculation in Topas. Each calculation has given both a size and a standard deviation. In all cases the sizes were approximately the same, so instead of listing all results, the results have been merged by these formulas:

$$\tilde{a} = \frac{\sum_{i=1}^{n} \frac{a_i}{(b_i)^2}}{\sum_{i=1}^{n} \frac{1}{(b_i)^2}} \quad \text{and} \quad \sim b = \sqrt{\frac{1}{\sum_{i=1}^{n} \frac{1}{(b_i)^2}}}$$

Where $a_i$ and $b_i$ are the size and standard deviation for measurement i, $\tilde{a}$ and $\sim b$ are the mean value of size and standard deviation for all the measurements of that vial.

LNE

The sizes reported by LNE are based on averages of n analysis on different vials (vial number not given).

## 3.6 Results

### 3.6.1 TiO2

Figures 3-6 and 3-7 shows the X-ray diffractograms of the titania samples and the results from the various crystallite size analyses from NRCWE and IMC-BAS are summarized in Tables 3-4 to 3-10. LNE contributed with phase identification of NM103, NM104 and NM105 as well as crystallite size and phase proportions of NM105.

The X-ray diffractograms shows good agreement between the results from IMC-BAS and NRCWE.

*Table 3-3 Crystallite sizes (nm) determined from measurements on NM100, Anatase*

| Vial | LNE | IMC-BAS | | | NRCWE | | |
| | Scherrer Equation | Peak fit, FWHM vs standard | Topas 4.2, standard less | Fullprof, quartz standard | Scherrer Equation | Topas 4.1, IB | Topas 4.1, FWHM |
|---|---|---|---|---|---|---|---|
| 0006+0007 | | | | | > 100 | > 100 | > 100 |
| 0016 | 141.2 | | | | | | |
| 0079 | | | | | | | |
| 0081 | | 56.66$^€$ | 61.87$^€$ (2.23) | 168.18$^€$ (1.9) | | | |
| 0083 | | | | | | | |
| 0211+0213+0214 | | | | | > 100 | > 100 | > 100 |
| 0406+0408 | | | | | > 100 | > 100 | > 100 |

$^€$ Average of three samples.

Co-funded by
the Health Programme
of the European Union

**The Anatase samples, NM100, NM101, NM102 and NM105**



*Figure 3-4 The diffraction data from NRCWE and IMC-BAS. Overall the data are very alike. The long measurements are done at IMC-BAS and the short ones at NRCWE.*

*Table 3-4 Crystallite sizes (nm) determined from measurements on NM101, Anatase*

| Vial | LNE Scherrer Equation | IMC-BAS | | | NRCWE | | |
| | | Peak fit, FWHM vs standard | Topas 4.2, standard less | Fullprof, quartz standard | Scherrer Equation* | Topas 4.1, IB | Topas 4.1, FWHM |
|---|---|---|---|---|---|---|---|
| 0180 | | | | | 7.0 ± 0.8 | 7.1 ± 0.2 | 10.0 ± 0.3 |
| 0239 | | | | | 6.9 ± 0.7 | 7.7 ± 0.2 | 10.8 ± 0.2 |
| 0415 | | | | | 7.2 ± 1.1 | 7.0 ± 0.1 | 9.8 ± 0.2 |
| 0510 | no data | | | | 6.5 ± 0.8 | 7.1 ± 0.1 | 9.9 ± 0.2 |
| 0729 | | | | | 6.9 ± 0.7 | 7.2 ± 0.1 | 10.1 ± 0.2 |
| 1266 | | | 5.30$^{€}$ (1.46) | 6.84$^{€}$ (0.95) | | | |
| 1268 | | 5.00$^{€}$ | | | | | |
| 1270 | | | | | | | |

$^{€}$ Average of three samples ; * Based on reflections: 101, 200, 105, 211, 116 and 220

*Table 3-5 Crystallite sizes (nm) determined from measurements on NM102, Anatase*

| Vial | LNE Scherrer Equation | Peak fit, FWHM vs standard | IMC-BAS Topas 4.2, standard less | Fullprof, quartz standard | NRCWE Scherrer Equation* | Topas 4.1, IB | Topas 4.1, FWHM |
|------|------|------|------|------|------|------|------|
| 0012 | 30.4 | | | | | | |
| 0092 | | | 15.81$^€$ (0.98) | 18.03$^€$ (5.0) | | | |
| 0094 | | 17.5$^\$$ | | | | | |
| 0095 | | | | | | | |
| 0121 | | | | | 22.7 ± 5.1 | 25.4 ± 1.4 | 28.0 ± 1.4 |
| 0477 | | | | | 23.0 ± 3.7 | 25.3 ± 1.4 | 27.5 ± 1.4 |
| 1000 | | | | | 23.5 ± 5.1 | 26.8 ± 1.6 | 29.0 ± 1.5 |

$^\$$ Average of two samples not specified. $^€$ Average of three samples ; * Based on reflections: 101, 200, 105, 211, 116 and 220
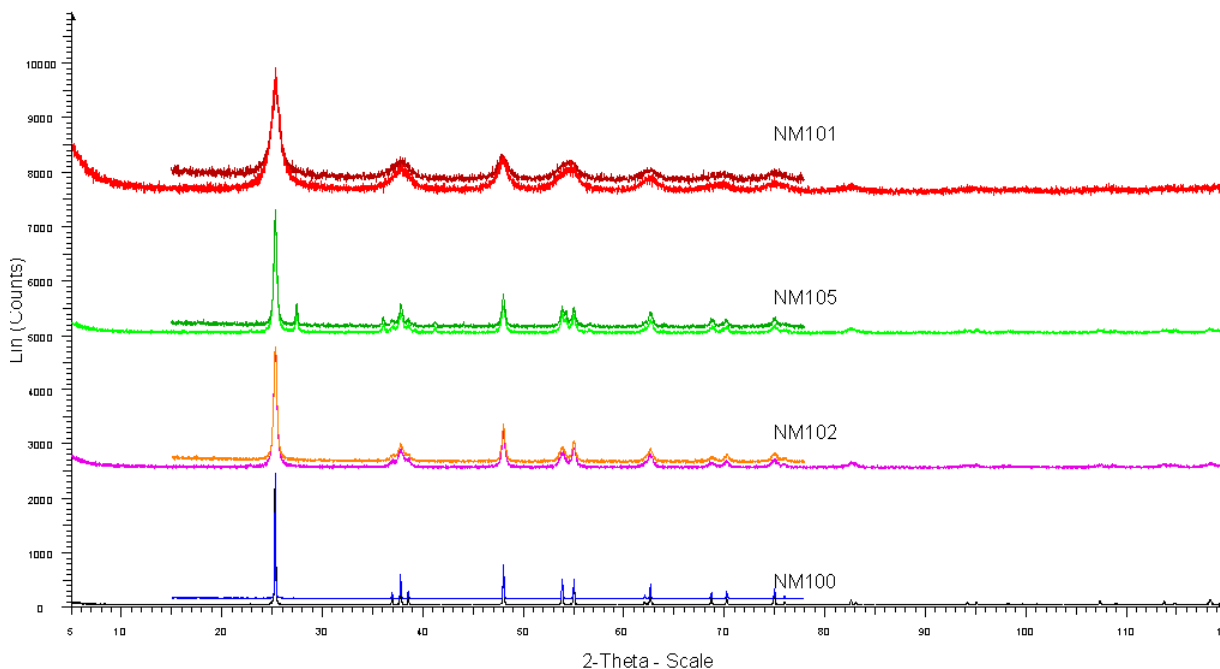
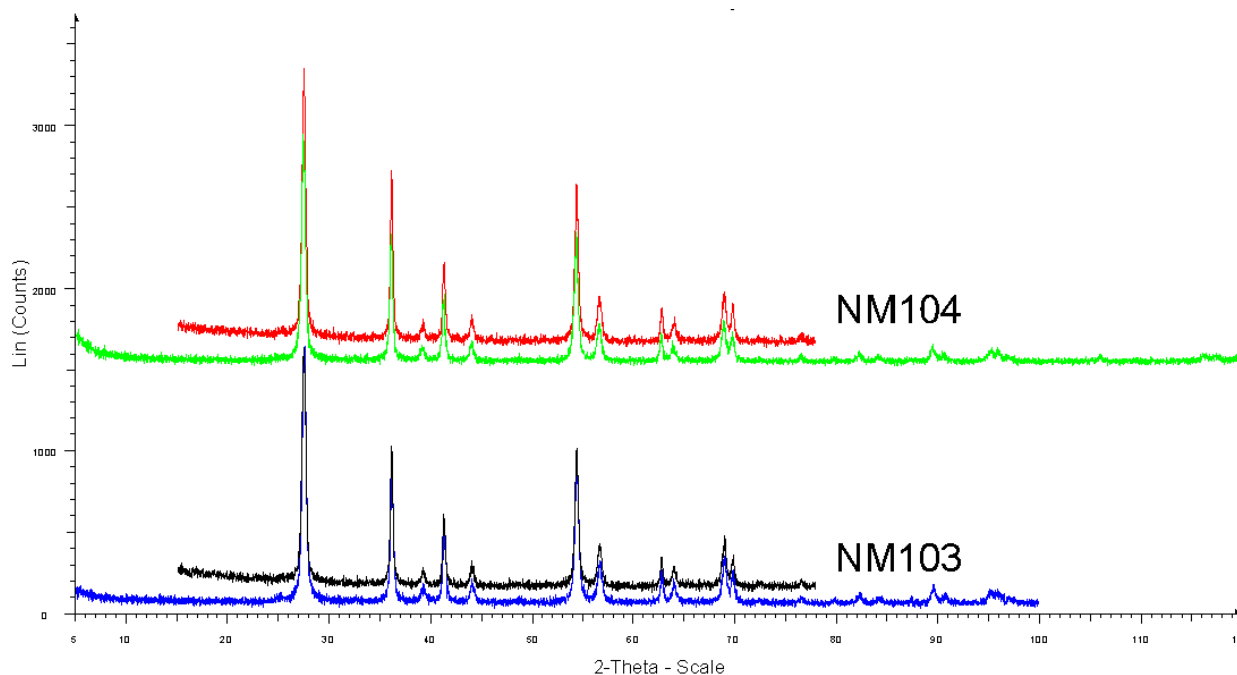**The Rutile samples, NM103 and NM104**



*Figure 3-5 Diffraction data from NRCWE and IMC-BAS. Again the data are very alike. The long measurements are done at IMC-BAS and the short ones at NRCWE.*

*Table 3-6 Crystallite sizes (nm) determined from measurements on NM103, Rutile[£].*

| Vial | LNE Scherrer Equation | IMC-BAS Peak fit, FWHM vs standard | Topas 4.2, standard less | Fullprof, quartz standard | NRCWE Scherrer Equation* | Topas 4.1, IB | Topas 4.1, FWHM |
|---|---|---|---|---|---|---|---|
| 0223 | | | | | 25.9 ± 5.6 | 25.4 ± 1.8 | 28.4 ± 1.9 |
| 0541 | | | | | 25.4 ± 4.7 | 24.7 ± 1.7 | 27.5 ± 1.7 |
| 0547 | 17.6 | | | | | | |
| 0615 | | | 19.42[€] | 18.03[€] | | | |
| 0617 | | | (1.03) | (5.9) | | | |
| 0618 | | | | | | | |
| 2097 | | | | | 26.7 ± 4.5 | 25.0 ± 1.7 | 27.8 ± 1.7 |

[€] Average of three samples ; * Based on reflections: 101, 200, 105, 211, 116 and 220; [£] LNE also only identified rutile in the sample.

*Table 3-7 Crystallite sizes (nm) determined from measurements on NM104, Rutile*

| Vial | LNE Scherrer Equation | IMC-BAS Peak fit, FWHM vs standard | Topas 4.2, standard less | Fullprof, quartz standard | NRCWE Scherrer Equation* | Topas 4.1, IB | Topas 4.1, FWHM |
|---|---|---|---|---|---|---|---|
| 0228 | | | | | 27.5 ± 3.1 | 24.9 ± 1.0 | 29.1 ± 1.1 |
| 0416 | | | | | 27.0 ± 3.3 | 24.7 ± 0.9 | 28.7 ± 1.1 |
| 0440 | | | | | 26.5 ± 3.5 | 24.4 ± 0.9 | 28.5 ± 1.0 |
| 0451 | 22.6 | | | | | | |
| 0529 | | | 19.52[€] | 18.43[€] | | | |
| 0530 | | 19.33[€] | (0.89) | (5.5) | | | |
| 0533 | | | | | | | |

[€] Average of three samples ; * Based on reflections: 101, 200, 105, 211, 116 and 220; [£] LNE also only identified rutile in the sample.

Conclusion on the TiO$_2$ samples

The size data from all the TiO$_2$ samples are summarized Table 3-10. For clarity the numbers have been rounded to nearest natural number and standard deviations are not listed due to the general consideration that the true standard deviation is on the order of 5 nm. The calculated sizes for the Rutile phase in NM105 are not listed either, as this is the minor phase and the size therefore is more uncertain. Most programs for calculations on powder diffraction data underestimate the error.

Of all samples, the data for NM100 stands out. According to the supplier the crystal size is between 200 nm and 220 nm. The data from NRCWE and the Fullprof data from IMC-BAS conclude that the crystals are large, but XRD size data should not be used if the calculated sizes exceed 100 nm. The Peak fit and TOPAS from IMC-BAS finds a crystal size around 60 nm, which is much smaller than

20

Co-funded by the Health Programme of the European Union

expected. As the datasets used for the calculations at IMC-BAS are the same, there is no obvious explanation for this difference.

*Table 3-8 Crystallite sizes (nm) determined from measurements on NM105, Anatase*

| Vial | LNE Scherrer Equation | Peak fit, FWHM vs standard | IMC-BAS Topas 4.2, standard less | Fullprof, quartz standard | NRCWE Scherrer Equation* | Topas 4.1 Ratio | Topas 4.1, IB | Topas 4.1, FWHM |
|---|---|---|---|---|---|---|---|---|
| 0051 | | | | | 27.7 ± 1.4 | 88.4 ± 0.2 | 27.9 ± 1.1 | 31.6 ± 1.2 |
| 0058 | | | | | 27.2 ± 0.9 | 88.3 ± 0.2 | 26.8 ± 1.0 | 30.8 ± 1.1 |
| 0078 | | | | | 26.0 ± 1.0 | 88.2 ± 0.2 | 26.9 ± 1.1 | 30.8 ± 1.2 |
| 2135 | | | | | 27.5 ± 1.0 | 88.6 ± 0.2 | 27.3 ± 1.1 | 31.7 ± 1.2 |
| 2167 2168 2171 2175 | 22.5 | | | | | | | |
| 2242 2244 2247 | | 18[€] | 18.15[€] (0.93) | 19.19[€] (2.1) | | | | |

[§] All identified NM105 to be a mixture of Anatase and Rutile. The size results are given for each polymorph. The anatase:rutile ratio is determined to be 86.36:13.64 (IMC-BAS) and 81±5:19±5. (LNE)
[€] Average of three samples; * Based on reflections: 101, 104, 200, 105 and 211.

*Table 3-9 Crystallite sizes (nm) determined from measurements on NM105, Rutile[§]*

| Vial | LNE Scherrer Equation | Peak fit, FWHM vs standard | IMC-BAS Topas 4.2, standard less | Fullprof, quartz standard | NRCWE Scherrer Equation# | Topas 4.1, IB | Topas 4.1, FWHM |
|---|---|---|---|---|---|---|---|
| 0051 | | | | | 68.0 ± 9.5** | 112 ± 31* | 156 ± 44* |
| 0058 | | | | | 62.2 ± 9.7** | 84 ± 15* | 117 ± 21* |
| 0078 | | | | | 60.0 ± 7.0** | 82 ± 16* | 115 ± 23* |
| 2135 | | | | | 57.0 ± 9.0** | 74 ± 15* | 104 ± 21* |
| 2167 | 39.5 | | | | | | |
| 2242 2244 2247 | | 23[€] | 26.79[€] (3.92) | 36.38[€] (24.2) | | | |

[§] All identified NM105 to be a mixture of Anatase and Rutile. The size results are given for each polymorph. The anatase:rutile ratio is determined to be 86.36:13.64 (IMC-BAS) and 81.5:18.5. (LNE) [€] Average of three samples; * Based on reflections: 101, 104, 200, 105 and 211. [*] These numbers are high and most likely not correct. As this is a minor phase the reflections are not very high, thus errors in determining the background and height of the reflections will have a large impact on the determination of IB or FWHM. [**] There are large deviations from reflex to reflex.

For all the other samples the difference between the highest calculated size and the lowest is smaller than 10 nm. The calculated sizes from NRCWE are in all cases larger than those from IMC-BAS. This is ascribed to differences in instrumental performance and the calculation procedures used. However, almost all the differences can be covered by the estimated 5 nm real standard deviation in the analysis.

*Table 3-10 Summary of XRD sizes calculated for $TiO_2$ using various instruments and principles.*

| | NM100[€] | NM101 | NM102 | NM103 | NM104 | NM105 (Anatase) |
|---|---|---|---|---|---|---|
| **Supplier information** | 200 - 220 | < 10 | - | 20 | 20 | 21 |
| **IMC-BAS Peak fit** | 57 | 5 | 18 | - | 19 | 18 |
| **IMC-BAS TOPAS** | 62 | 5 | 16 | 19 | 20 | 18 |
| **IMC-BAS Fullprof** | 168 | 7 | 18 | 20 | 18 | 19 |
| **NRCWE Scherrer eq.** | > 100 | 7 | 23 | 26 | 27 | 27 |
| **NRCWE TOPAS, IB** | > 100 | 7 | 26 | 25 | 25 | 27 |
| **NRCWE TOPAS, FWHM** | > 100 | 10 | 28 | 28 | 29 | 31 |
| **LNE Scherrer eq.** | 141 | - | 30 | 18 | 23 | 23 |

[€] Size-data not reliable due to large crystallite size.

## 3.6.2 SAS

For the silica analysis, IMC-BAS used standard sample holders and has only observed the expected amorphous "pattern". They analyzed samples from vial 0156 and 0157 (NM200), vial 0100 and 0102 (NM201), vial 0104 and 0108 (NM202), vial 0280 and 0282 (NM203), and no vials of NM204.

NRCWE were mounted the samples vacuum grease in a Si low background sample holder. In these data crystalline impurities of $Na_2SO_4$ and/or boehmite and/or cristobalite and potentially also graphite were observed in NM200, NM201, NM203, but not in NM204. The pure vacuum grease was confirmed to contain no crystalline impurities. Occasional presence of $Na_2SO_4$ was indicated by producer as an impurity from the production line and observed by presence three 3 reflections in the X-ray diffractograms.

Both types of mounting have advantages and disadvantages. When mounting in a standard sample holder, as done by IMC-BAS, one is sure only to measure the sample. However, as some of the material may "jump out" of the sample holder, it can not be known, whether impurities are lost or not. The strength of the vacuum grease method is that if only a thin layer of sample is dropped on the sample holder, all the material stick to the holder, and all of it is measured.

Due to the low impurity contents and to investigate the potential presence of other phases, NRCWE conducted a series of repeated analysis. The results from these tests are summarized in Tables 3-11 to 3-14, where we summarize the number of analysis resulting in observation of the different phase reported compositions. It should be noted that this is not a statistical comparison. Due to the random detection, the phases are thought to be inhomogeneously distributed in the powders and when not observed they may be present in concentrations below the detection limit of the method.

*Table 3-11. Results of NRCWE XRD impurity analysis on NM200 with notation on the number of analysis and times different phase combinations were observed.*

| Content | n Observations | Vial 0072 | Vial 0441 |
|---|---|---|---|
| Amorphous | 0 | | |
| Amorphous + $Na_2SO_4$ | 3 | 2 | 1 |
| Amorphous + $Na_2SO_4$ + "Boehmite" (AlO(OH)) | 4 | 3 | 1 |
| Amorphous + $Na_2SO_4$ + "Cristobalite" ($SiO_2$) | 1 | 1 | |
| Total number | 8 | 6[€] | 2 |

[€] One normal XRD scan range and 5 very narrow scan ranges for identification of specific impurity phases

*Table 3-11. Results of NRCWE XRD impurity analysis on NM201 with notation on the number of analysis and times different phase combinations were observed.*

| Content | n Observations | Vial 0022 | Vial 0444 |
|---|---|---|---|
| Amorphous | | | |
| Amorphous + $Na_2SO_4$ | 3 | 2 | 1 |
| Amorphous + $Na_2SO_4$ + "Boehmite" (AlO(OH)) | 6 | 3 | 3 |
| Total number | 9 | 5 | 4 |

*Table 3-12. Results of NRCWE XRD impurity analysis on NM202. with notation on the number of analysis and times different phase combinations were observed.*

| Content | n Observations | Vial 0027 | Vial 0486 |
|---|---|---|---|
| Amorphous | 0 | | |
| Amorphous + $Na_2SO_4$ | 0 | | |
| Amorphous + $Na_2SO_4$ + "Boehmite" (AlO(OH)) | 5 | 3 | 2 |
| Total number | 5 | 3 | 2 |

*Table 3-13. Results of NRCWE XRD impurity analysis on NM203 with notation on the number of analysis and times different phase combinations were observed.*

| Content | n Observations | Vial 0152 | Vial 0363 |
|---|---|---|---|
| Amorphous | 3 | 2 | 1 |
| Amorphous + $Na_2SO_4$ | 0 | | |
| Amorphous + "Boehmite" (AlO(OH)) | 3 | 1 | 2 |
| Total number | 6 | 3 | 3 |

No impurity phases were detected in NM204 and where powder from three vials were analyzed by IMC-BAS (vial 0098 and 0102) and one (vial 0006) was analyzed by NRCWE.

Conclusion on the SAS samples

The SAS samples are mainly amorphous, but the type of sample mounting seems to have a significant influence on what is seen from the XRD data. In the full sample holder used by IMC-BAS no impurities are detected, whereas the small samples on the low background Si-sample holders used by NRCWE show many impurities. The impurities could not be ascribed to the vacuum grease used to mount the samples on the Si sample holder in the NRCWE analysis. Results from the elemental analyses in chapter 5 further support the findings from the XRD analyses.

### 3.6.3  MWCNT

Analyses of raw powder MWCNT

IMC-BAS investigated the possibility to detect catalyst, carbon allotropes and the CNT structure by XRD on powders from NM400, NM401, and NM402. The X-ray diffractograms show one significant broad reflection and some smaller. All peaks were ascribed to reflections from the CNT. Besides CNT, graphite may be present in NM401. The CNT reflections were used to estimate the wall thickness based on the widths of the reflections. however, it should be strongly emphasized that there is not consensus on whether wall thickness can be properly calculated from X-ray diffractograms. The results are summarized in Table 3-15.

*Table 3-15. Results from the XRD size calculations on NM400, NM401 and NM402 by IMC-BAS.*

| Material | Size [nm] method | | |
|----------|------------------|---|---|
| CNT | XRD / peaks [1] | Rietveld [2] | Standard +Rietveld [3] |
| NM 400 | 2 | 2.832 (0.641) | 3.2(0.6) |
| NM 401 (+Graphite?) | 9 | 8.58 and 12.22 | 8.6 (for graphite 2H hkl 002 and 006) |
| NM 402 | 2 | 2.939 (2.061) | |

[1] Ognyan Petrov, peak fit, FWHM vs. standard peak ; [2] Louiza Dimova, Bruker Topas 4.2, standard less ; [3] Rosica Nikolova, Fullprof + quartz standard.

NRCWE, residual after TGA

NRCWE, attempted to assess the nature of the catalyst impurities by burning away the carbon material to leave behind the non-combustable residual inorganic catalyst material. In this way the signal to noise ratio should be increased. For convenience, this analyses was done on the residual after thermogravimetric analysis (TGA), which is presented in Chapter 4. The XRD analyses were performed on residuals after $1000^{\circ}$C combustion of powders from NM400, NM402, NRCWE006, and NRCWE007, where considerable residual masses were found after combustion.

The diffractograms are shown in Figure 3-8 to 3-11 and all show clear sharp peaks in the combusted MWCNT residuals. In NM400, the impurity was identified as $Al_2O_3$ or a closely related compound. In NM402, the crystalline material was $Fe_2O_3$. In NRCWE006, data were obtained without a

24

monochromator, thus the double reflections, especially seen at high angles (Figure 3-10). The main phase is $Fe_2O_3$, however there unidentified reflections were observed at $2\theta = 20$ and $35°$. The extra phase(s) could not be identified from this few reflections. In NRCWE, the residual contained $NiFe_2O_4$. These results are in good agreement with the major elemental impurities reported in Chapter 5.
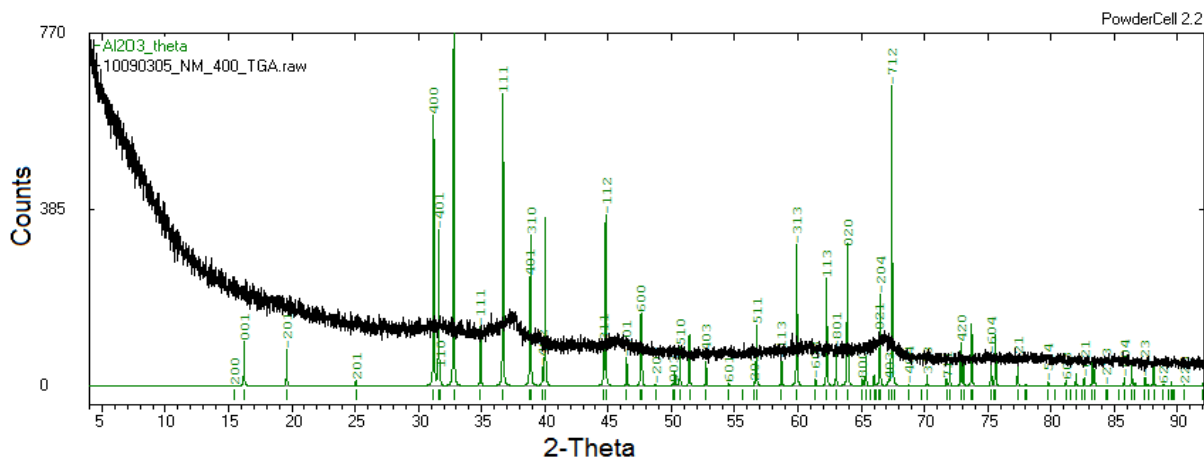
*Figure 3-6. NRCWE diffraction data on the residual of NM400 after heating to 1000 °C*
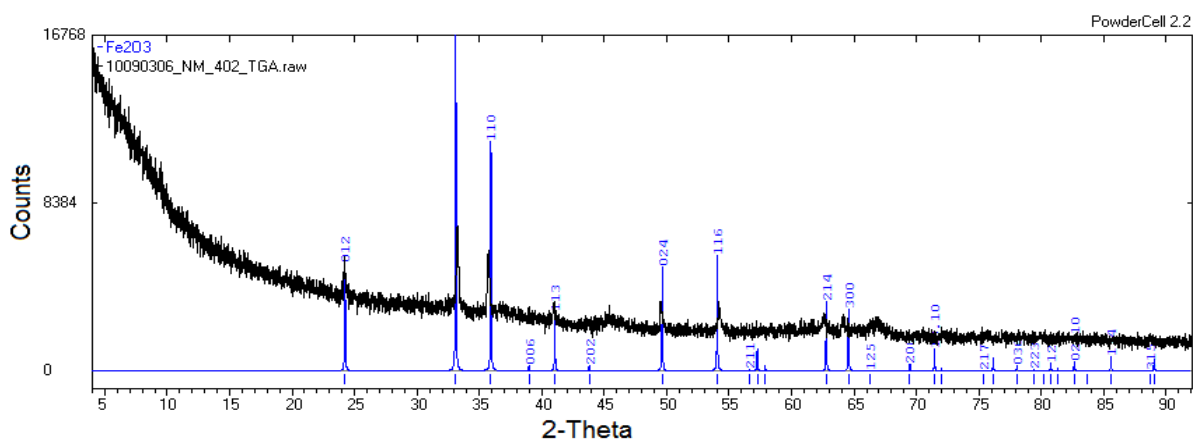


*Figure 3-7 NRCWE diffraction data on the residual of NM402 after heating to 1000 °C*
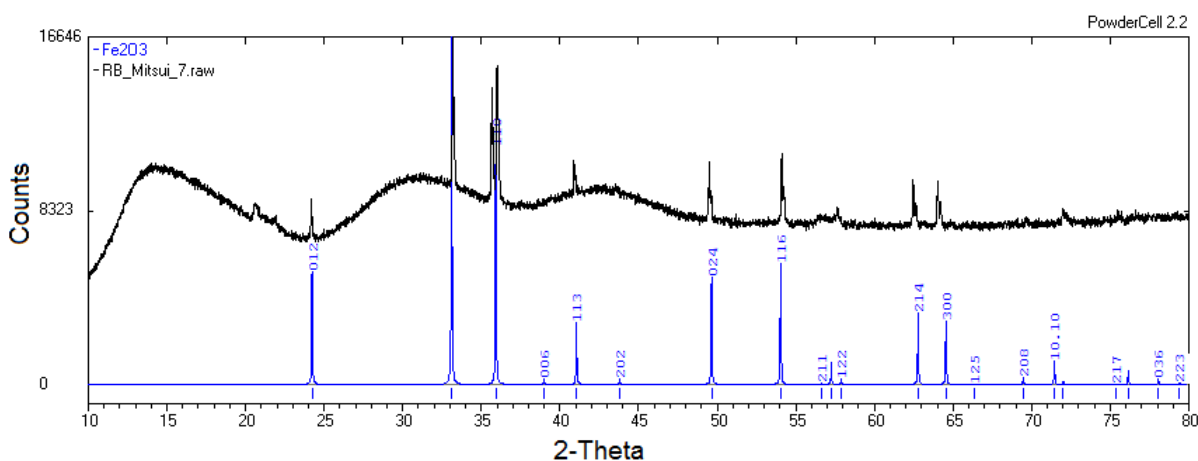


*Figure 3-8 NRCWE diffraction data on the residual of NRCWE006 after heating to 1000 °C*

*Figure 3-9 NRCWE diffraction data on the residual of NRCWE007 after heating to 1000 °C*


# 4  TGA and DTA analysis


Thermograviometric Analyses (TGA) were completed by NRCWE and supporting data was given by IMC-BAS using Differential Thermograviometric Analyses (DTA)

In a thermograviometric the mass of a sample is weighed as function of temperature during heating in typically air, $O_2$ or $N_2$. The mass-loss and decomposition temperatures give information about the sample, e.g. adsorbed water will evaporate around 100 °C, whereas most other associated or technically added organic coatings will evaporate or combust at higher temperatures.

For carbon nanotubes, the combustion pattern and combustion temperature may indicate the quality of the CNT and presence of other combustible matter. Decomposition in several steps will indicate a non-homogeneous sample containing several different types combustible compounds, which could in fact all be structurally different carbon nanotubes.

In DTA, the reference and the sample undergo identical thermal cycles; they are either heated or cooled with the same rate. The temperature is measured for both sample and reference, and the difference is calculated. Most transformations such as phase transitions, melting, crystallization, decomposition etc. are either endothermic or exothermic; that is they either require or release energy. Thus when such a transformation takes place the temperature of the material will deviate from a reference. This is what is seen by DTA.


## 4.1  Thermogravimetric analysis (TGA)

For the thermogravimetric analysis (TGA) NRCWE used a Mettler Toledo TGA/SDTA 851e and an oxygen atmosphere. The heating rate for the MWCNT was 2.5 K/min over a temperature range of 25 °C to 1000 °C. For all other NM the heating rate was 10 K/min from 25 °C to 1000 °C. The sample holders used for the TGA measurements were made of alumina and had a volume of 70 µL or 150 µL.

27

## *4.2  Differential gravimetric analysis (DTA)*

IMC-BAS used a STA781 and DTA 675 from Stanton Redcroft for the differential thermal analysis (DTA). The heating rate was 10 $^o$C/Min.

In all figures the black curve represents the gravimetric data, the red is the differential thermal data and the blue (only for NM104) is the first derivative of the gravimetric data.

## *4.3  Results*

The data are presented here for each sample with short comments of each measurement. The data are summarized in two summary tables at the end of the chapter.

### 4.3.1  The TiO$_2$ samples

Results of the TGA and DTA analyses on the titania samples are shown in Figures 4-1 to 4-9. In brief, For NM100, the weight change is due to buoyancy (Figure 4-1), whereas NM101 shows a significant mass loss up to ca. 100°C which is ascribed to trapped or adsorbed water (Figure 4-2). In this sample, a second episodic loss is observed at ca. 200°C, which is ascribed to associated organic matter or coating. Similar behavior is observed for NM104 (Figure 4-8).
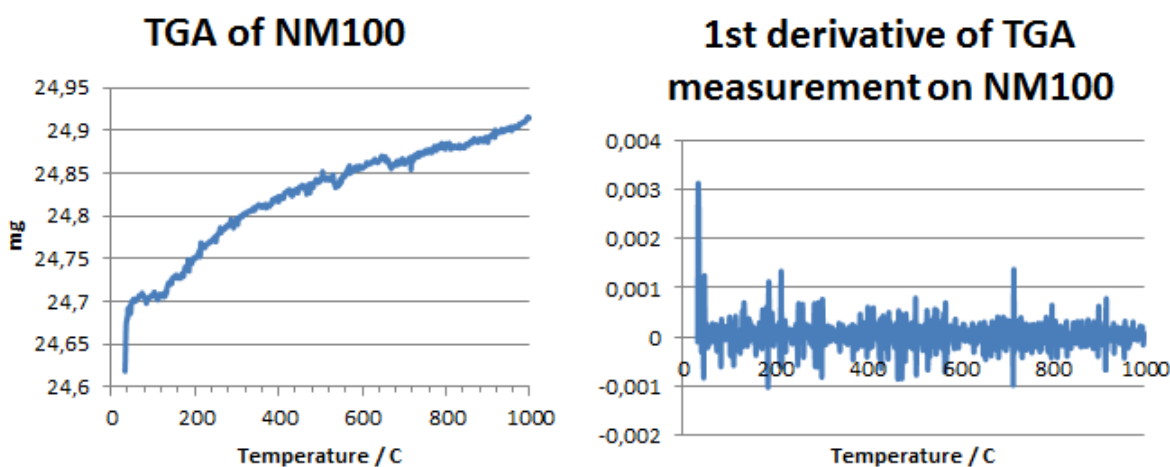


*Figure 4-1. Results from TGA measurement on NM100..*

For NM101, there are two weight losses. The first and greatest loss occurs below 100°C, and is most likely due to adsorbed water. The second weight-loss event occurs around 200°C and is most likely due to an organic coating or associated organic matter.
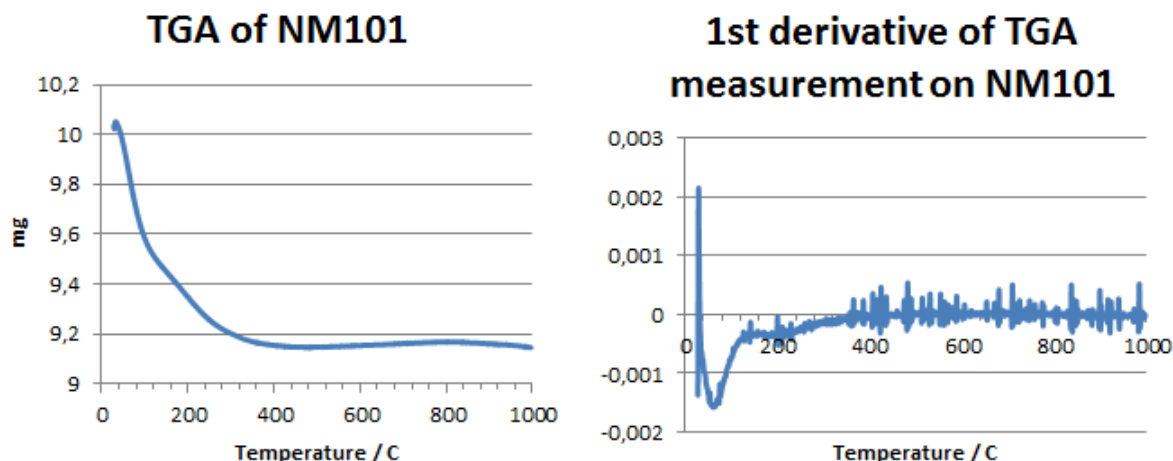
Figure 4-2. Results from TGA measurement on NM101.

The measurement of NM102 is very noisy due to problems with the instrument. However, it is concluded that there is no weight loss and the change in weight is due to buoyancy.
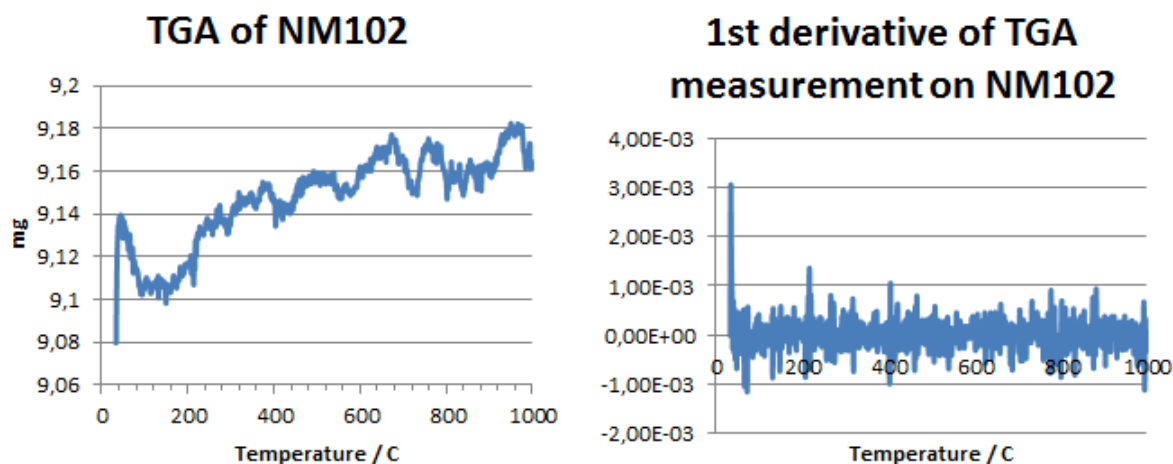


Figure 4-3. Results from TGA measurement on NM102.

For NM103, there is a small but gradual weight loss, which may in fact be due to evaporation/combustion in several steps. There appears to be a change in the slope around 200°C, but the measurement is noisy and it is difficult to be sure. However the weight loss is above 100°C and is most likely due to a coating. According to the DTA/TG results, there are no indications of any significant phase transformation.
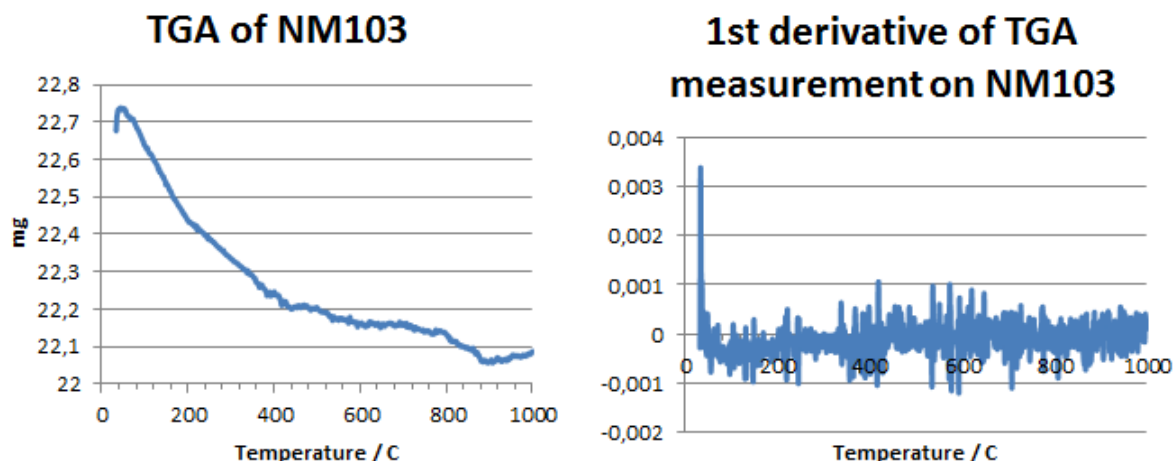
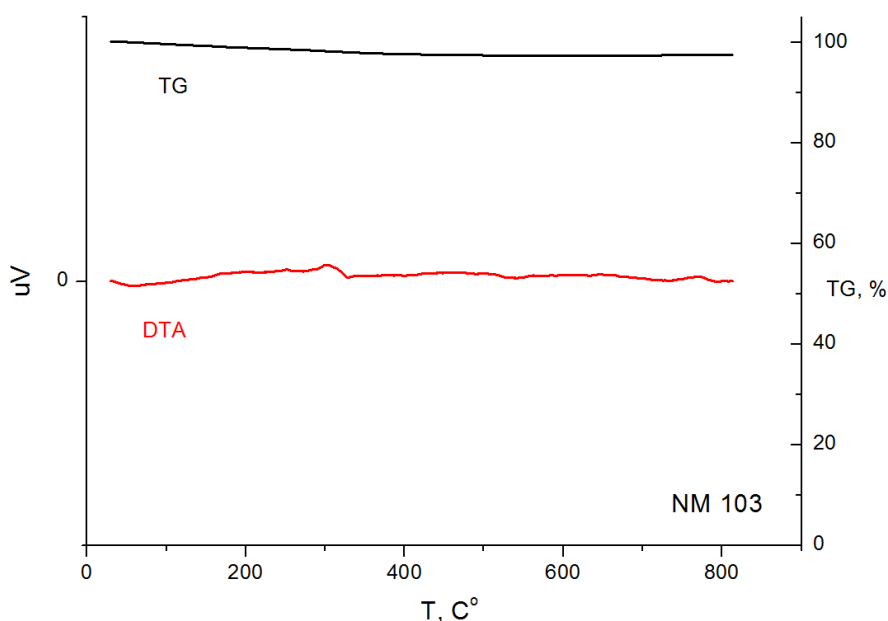Figure 4-4. Results from TGA measurement on NM103



Figure 4-5. DTA/TG results for sample NM103.

For NM104, there is a small gradual weight loss. It most likely occurs in two steps, as there appears to be a change in the slope around 200°C. The second weight loss is above 100°C and is most likely due to a organic coating or associated organics. According the DTA/TG results, the DTA curve for NM104 is shown on the top at the right. For the last weight loss around 320°C a peak is seen at the DTA curve indicating a phase transformation.
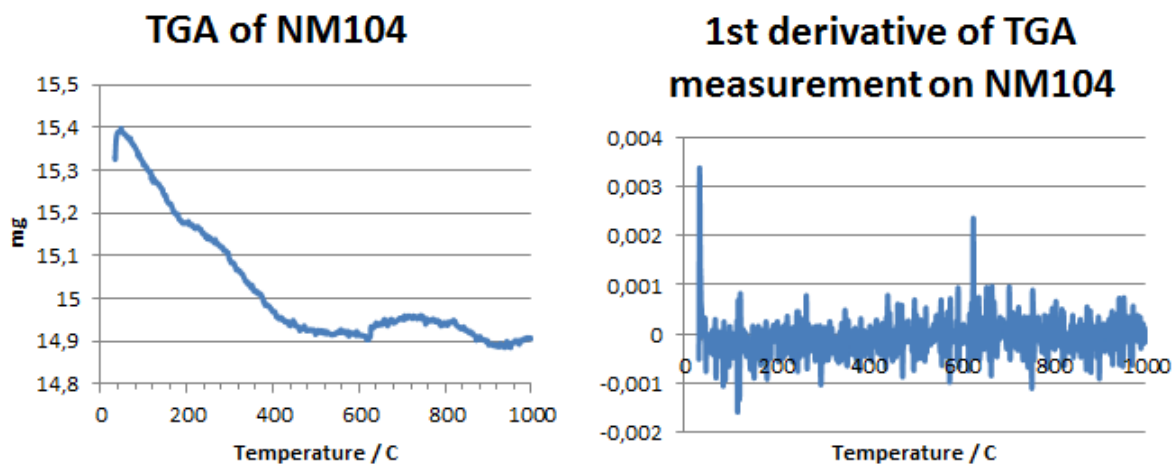
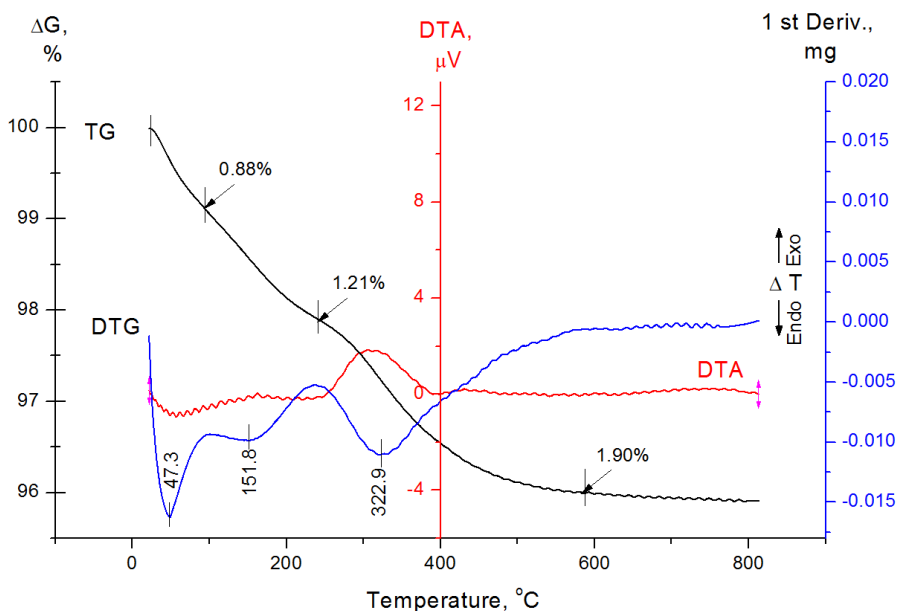*Figure 4-6. Results from TGA measurement on NM104.*



*Figure 4-7. DTA/TG results for sample NM104.*

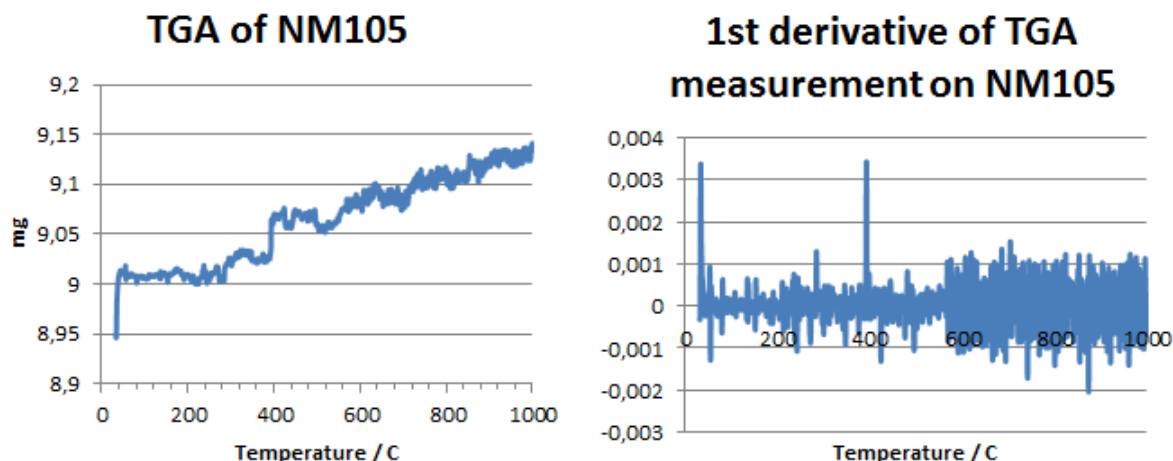For NM105, the change in weight is due to buoyancy and again this is a noisy measurement.
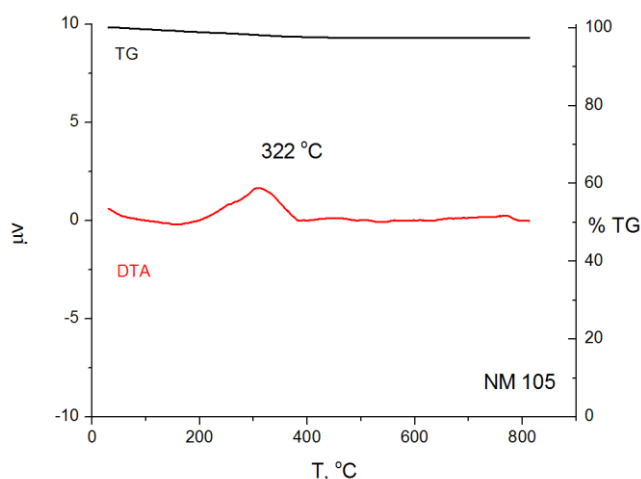
Figure 4-8. Results from TGA measurement on NM105.



Figure 4-9. DTA/TG results for sample NM105. A phase transformation is seen at the 322 °C.

## 4.3.2  The SAS samples

Figures 4-10 to 4-16 shows the results from thermogravimetric analyses of the synthetic amorphous silica NM. Weight losses below 100°C for NM200, NM201, and NM204 suggest that these samples contain adsorbed water. The same samples also have a gradual mass-loss up to ca. 200°C. This suggests presence of an organic compound, which may be functional coatings. The remaining NM202 and NM203 did not react thermograviometrically in the oxygen atmosphere suggesting presence of no organics.

For NM200, The first and most pronounced weight loss is below 100°C. It may be water attached to the surface. There is a second more gradual weight loss, possibly a coating.
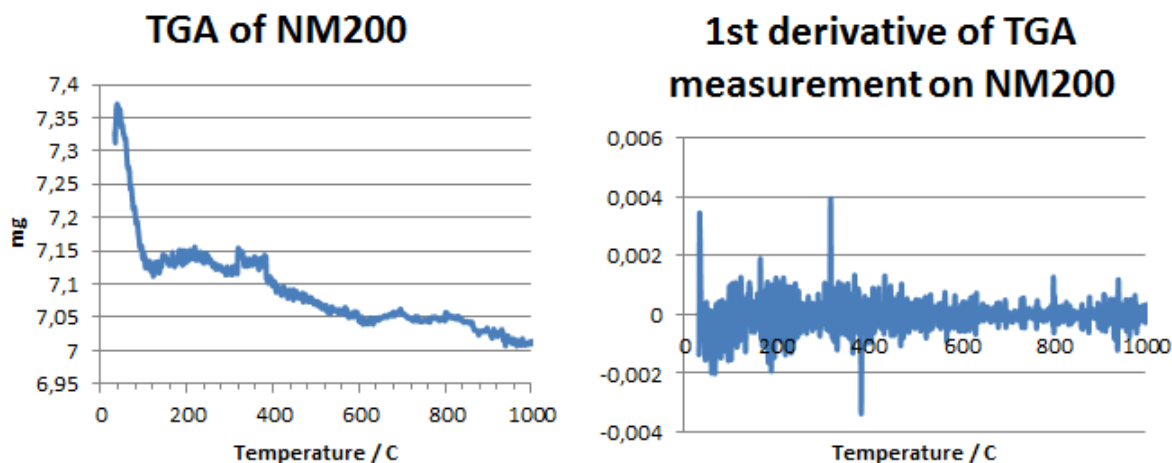
*Figure 4-10. Results from TGA measurement on NM200.*

For NM201, the first weight loss occurs below 100 °C. It may be water attached to the surface. There is a second more gradual weight loss, possibly a coating.



*Figure 4-11. Results from TGA measurement on NM201.*

For NM202, the change in weight is due to buoyancy. DTA/TG results for sample NM202 showing no indication of any phase transformations

## TGA of NM202



## 1st derivative of TGA measurement on NM202
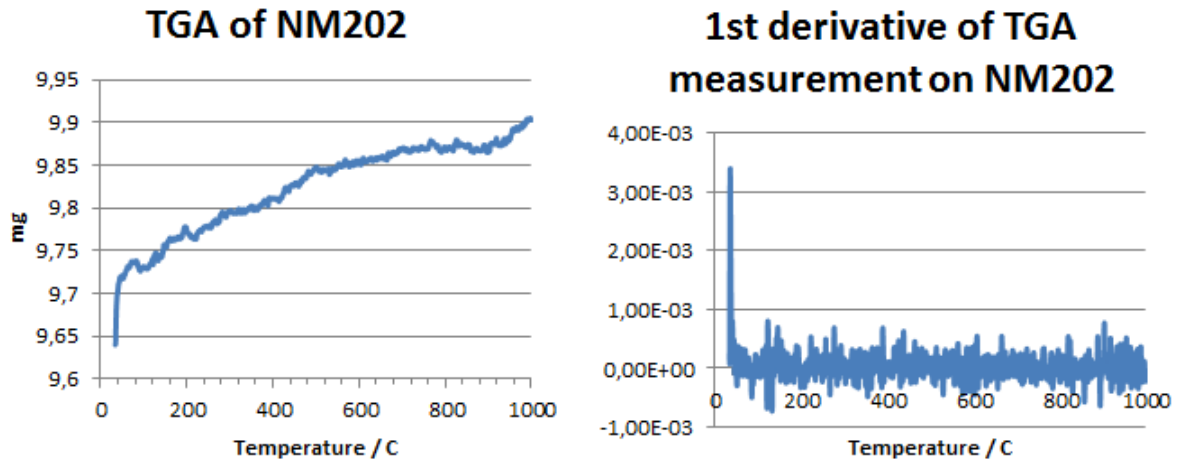
*Figure 4-12. Results from TGA measurement on NM202.*
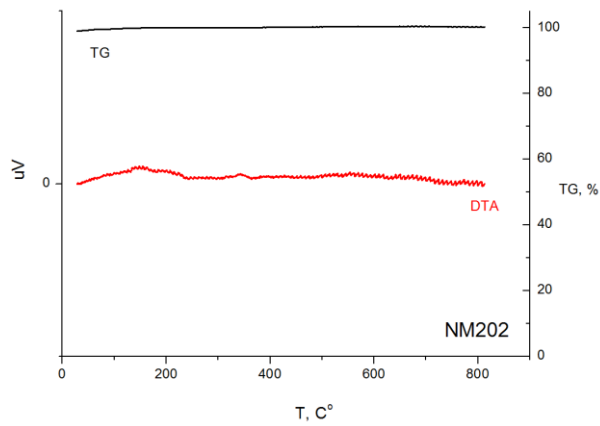


*Figure 4-13. DTA/TG results for NM202*

For NM203, the change in weight is due to buoyancy. DTA/TG results show a phase transformation at 324 °C.

*Figure 4-14. Results from TGA measurement on NM203. The change in weight is due to buoyancy.*



*Figure 4-15. DTA/TG results for sample NM203. There is a phase transformation at 324 °C.*

For NM204, results from TGA measurement show a first weight loss below 100 °C. It may be water attached to the surface. There is a second more gradual weight loss, possibly a coating.

35

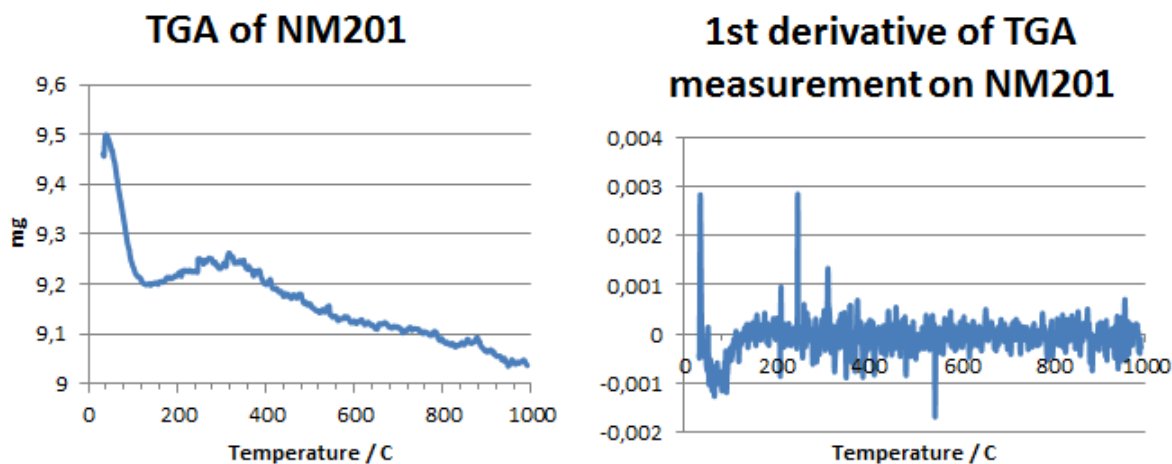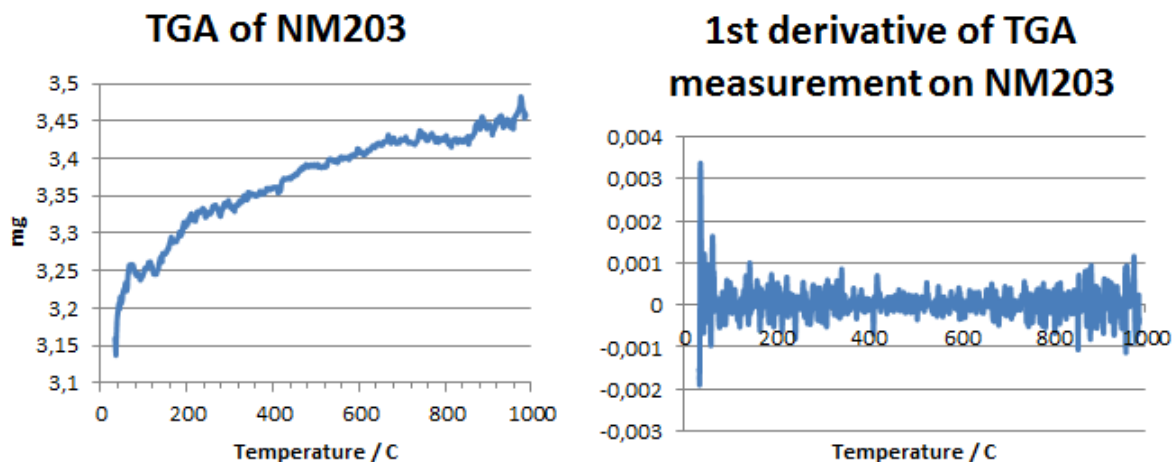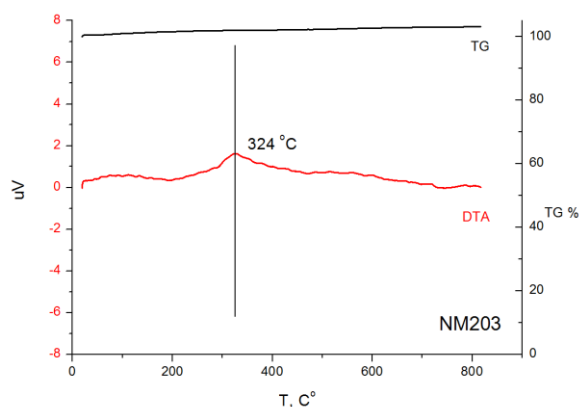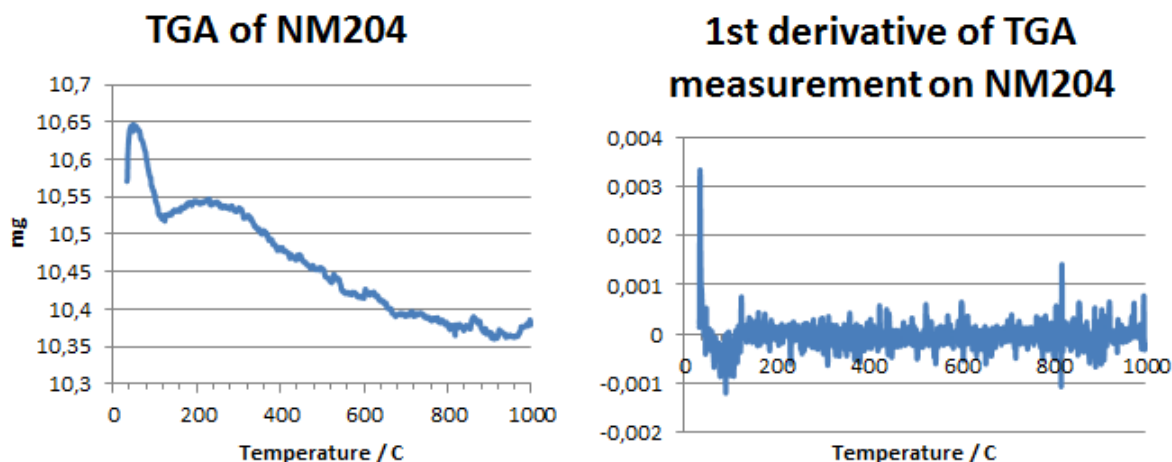*Figure 4-16. Results from TGA measurement on NM204*

### 4.3.3 The MWCNT samples

Figures 4-17 to 4-24 show the results from thermogravimetric analyses of MWCNT. In general, a thermogravimetric analysis on CNT is not straightforward due to inhomogeneous sample material. This results in different combustion patterns depending on sample size. However, most samples appear to produce reliable representative results between a few mg and up to more than 10 mg depending on the material. In one sample (NM402), the representative amount could not be clearly identified and may be larger than 13 mg. Only NM403 and NRCWE007 appears to be homogeneous materials, but noteworthy, the starting mass in tests of NM403 was also among the highest (ca. 14 mg) tested in the entire test (Figure 4-22).

NM400 is highly inhomogeneous as shown by the 3 different combustion curves (best seen on the 1st derivative), where the (small) green sample have one decomposition temperature and the red and blue have several – in different ratios – indicating different compounds.From these data it is seen, that a rather large sample, **more than 8 mg is needed to get a representative sample**. DTA/TG results for sample NM400 show a strong wide exothermic peak between 500 and 650C corresponding to the temperature range with high weight loss in TGA.
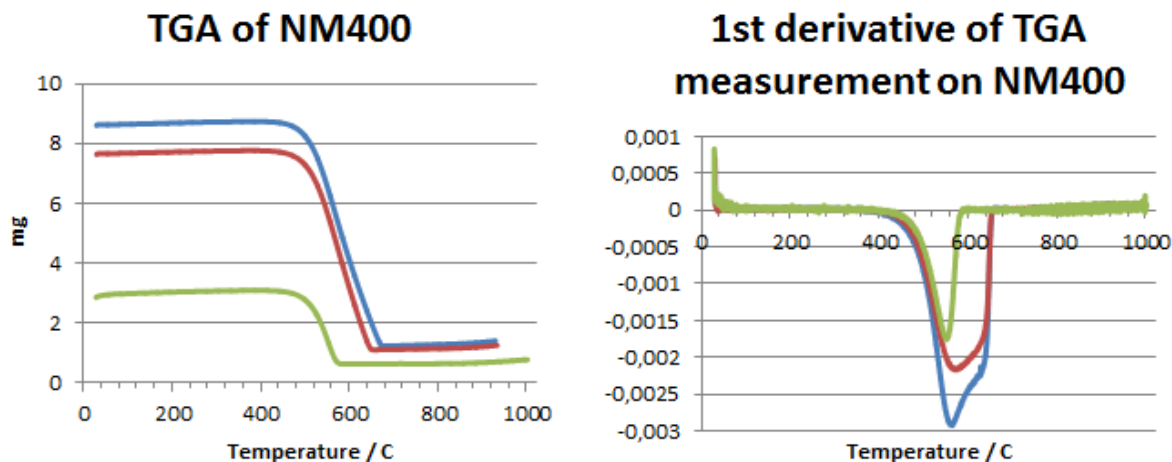
*Figure 4-17. Results from TGA measurement on NM400.*
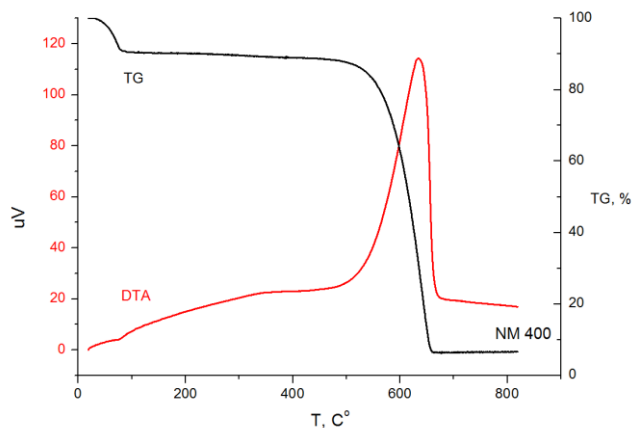


*Figure 4-18. DTA/TG results for sample NM400.*

The curves for the decomposition of different NM401 masses appear highly repeatable and indicate an homogenous NM. The decomposition temperature is approximately the same for all runs. However when considering the residual, there is much catalyst in the samples and a large variation in how much catalyst is present. From this perspective, the sample appears inhomogenous and **at least 4 mg is estimated to get a representative sample**. The DTA/TG results for show a strong exothermic reaction peaking at ca. 750C corresponding well to the TGA data by NRCWE.
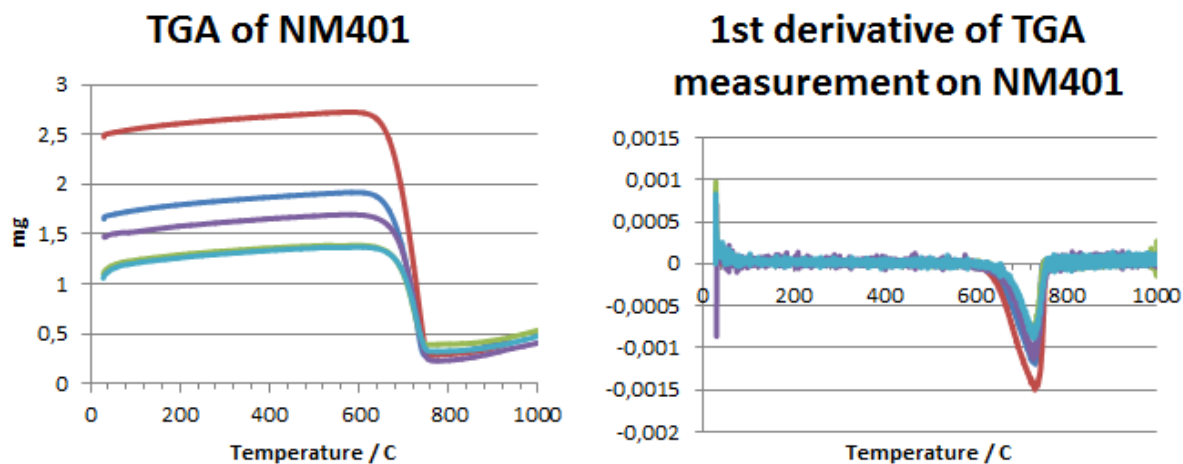
*Figure 4-19. Results from TGA measurement on NM401.*
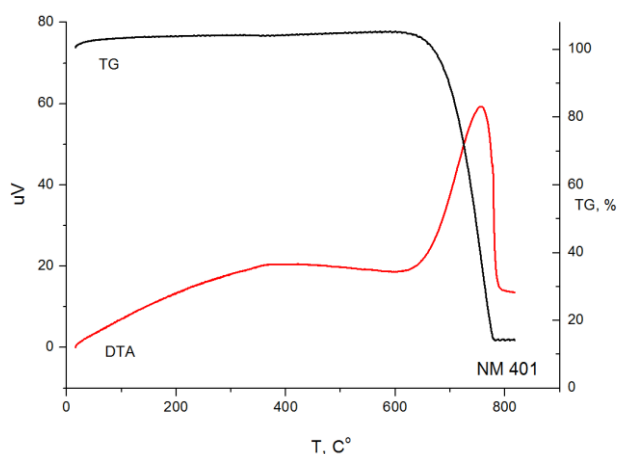


*Figure 4-20. DTA/TG results for sample NM401.*

The Results from TGA measurements on NM402 show the signature of an inhomogeneous sample. The 3 curves are all different (best seen on the 1st derivative), where the (small) green sample have one decomposition temperature and the red have two and the blue has several. From these data it is seen, that a large sample, **more than 13 mg is needed to get a representative sample**.
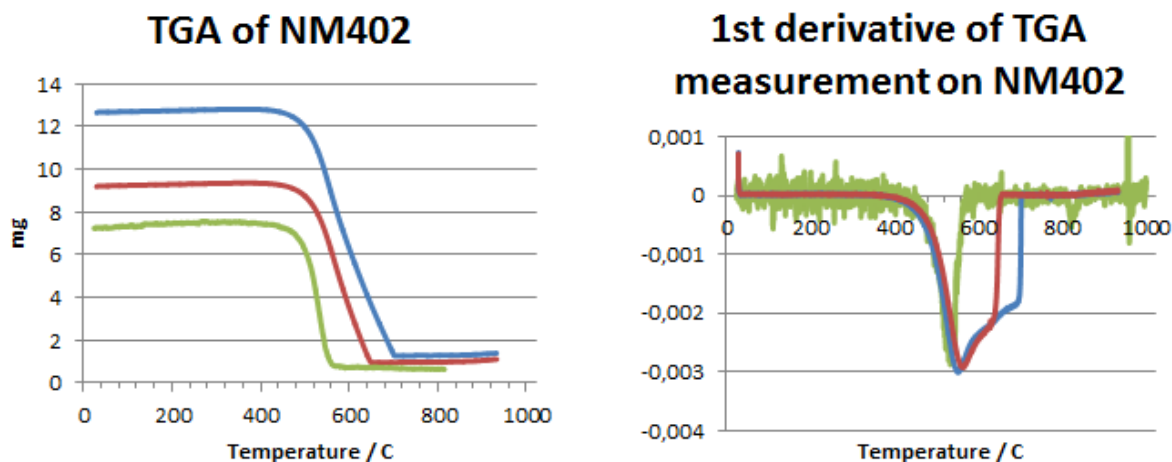
*Figure 4-21. Results from TGA measurements on NM402*

NM403 is a very uniform sample. The "strange" form of the curves, marked by the arrow is spontaneous combustion.
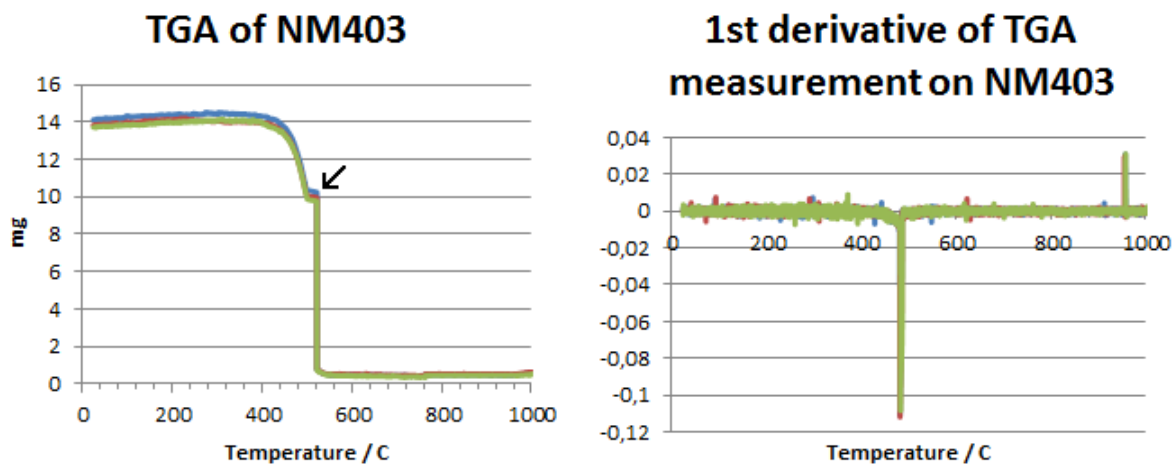


*Figure 4-22. Results from TGA measurement on NM403.*

NRCWE006 appears quite inhomogeneous, though some of the differences in decomposition temperature might be explained by very different amounts of catalyst. The notch in the purple curve is an instrumental error.
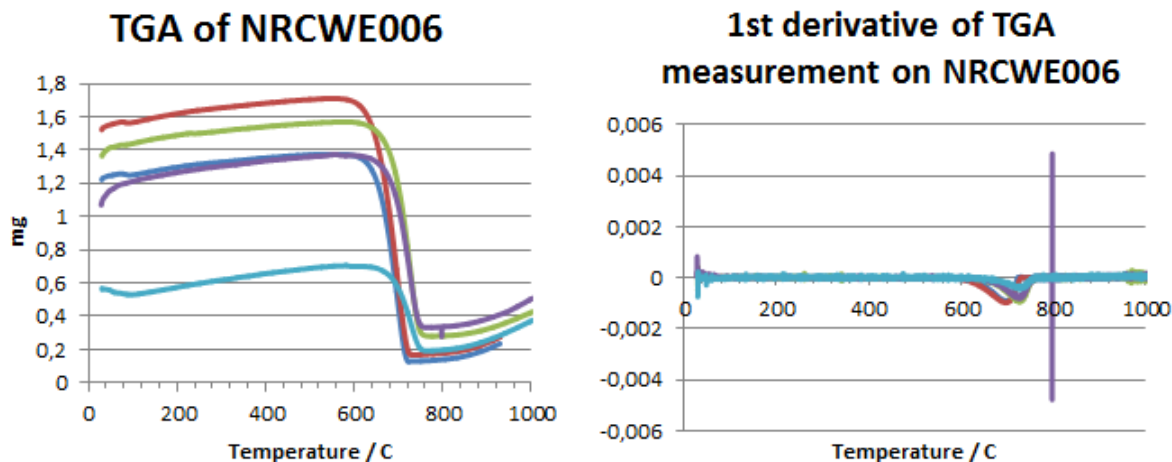
*Figure 4-23. Results from TGA measurement on NRCWE006.*

There is much noise in the green TGA measurement on NRCWE007. The green curve for the first derivative has been rescaled, not to cover the data for the other measurements. The measurements show a fairly homogeneous sample with similar combustion pattern from ca. 5 to 9 mg.
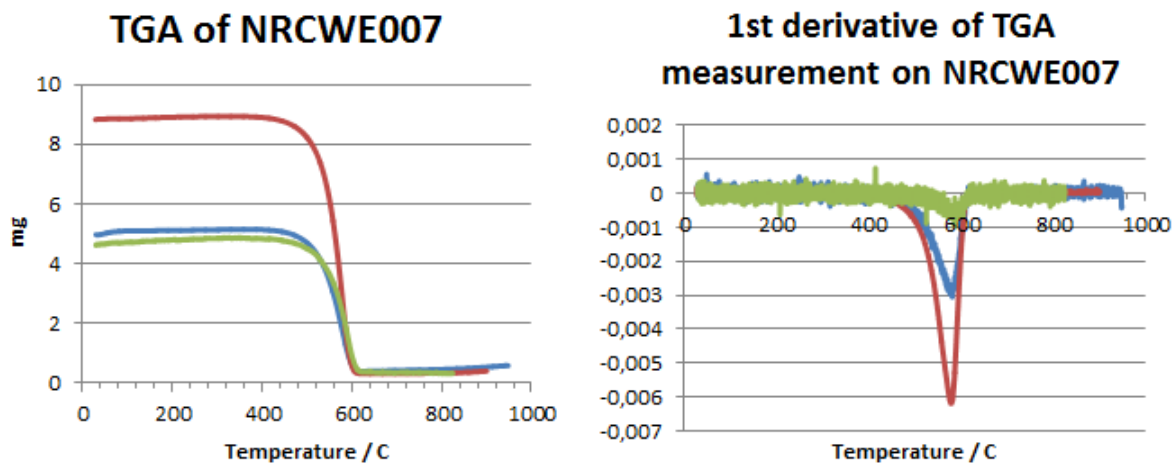


*Figure 4-24. Results from TGA measurement on NRCWE007.*

## 4.4 Summary of thermogravimetric analysis

TGA measurements on the TiO$_2$ and SAS samples were all performed only once. Except for NM203 the quantities analyzed were sufficiently large to be representative, and the main purpose for the measurements was to detect presence of coating on the materials.

TGA measurements on the MWCNT were completed several times for each sample. By doing so, the data can be used for several purposes. Unlike the TiO$_2$ and the silica samples, the MWCNT are not necessarily homogeneous; neither in concentrations of carbon and catalyst impurities, nor in the dimensions and qualities of the individual tubes. Inhomogeneity in carbon allotropes and tube characteristics will result in different combustion profiles. By several measurements, the amount of catalyst can be determined from a larger volume. By comparing the measurements, one can evaluate the homogeneity of the sample and give an estimate of how much sample is required to have a "representative sample" as discussed above.

For further use, the key results on coatings and purity of CNT is summarized in Tables 4-1 and 4-2, respectively.

Table 4-1. TGA data used for estimating the amount of coating in the TiO$_2$ and SAS samples.

| Sample | Coating | Weight of coating (wt%) |
|--------|---------|-------------------------|
| NM-100 | N | - |
| NM-101 | Y | 8 |
| NM-102 | N | - |
| NM-103 | Y | 2 |
| NM-104 | Y | 2 |
| NM-105 | N | - |
| NM-200 | Y (H2O?) | 3 |
| NM-201 | Y (H2O?) | 3 |
| NM-202 | N | - |
| NM-203 | N | - |
| NM-204 | Y | 0.5 |

Table 4-2 TGA results on the amount of impurities in the MWCNT samples.

| Sample | Appear homogenous | Weight Catalyst (%) | Main decomposition temperature (°C) |
|--------|-------------------|---------------------|-------------------------------------|
| NM-400 | N | 16.2 ± 2.9 | 563 ± 8 |
| NM-401 | N | 18.1 ± 6.7 | 729 ± 2 |
| NM-402 | N | 10.6 ± 0.4 | 555 ± 9 |
| NM-403 | Y | 3.2 ± 0.3 | 482 ± 1 |
| NRCWE-006 (Mitsui) | (Y) | 17.6 ± 7.2 | 714 ± 14 |
| NRCWE-007 (Cheap Tubes) | Y | 6.2 ± 1.9 | 582 ± 3 |

# 5 Elemental composition

The elemental composition of any powder or dispersed material is essential information for categorization of the substance; evaluate the potential presence of inorganic coatings, catalysts and un-intended impurities all to be linked with the associated material toxicity. The elemental composition may be analyzed using a range of different techniques and given in different data qualities ranging from qualitative to fully quantitative analysis. In this work three different analyses were performed, including energy dispersive X-ray spectroscopy (EDS or EDX) on powder tablets and inductive coupled plasma (ICP) with mass (MS) or optical emission spectrometry (OES) for detection and quantification on extracted elements. In the analyses, the extraction methods to analyze CNT and determination of the impurities therein had major focus. Details of the applied techniques are described below.

## 5.1 Analytical procedures

### 5.1.1 EDS

EDS is short for Energy-dispersive X-ray spectroscopy and may be available as an extra analytical tool in electron microscopes.

The analysis is based on the fact that when hitting a material with charged particles, such as an electron beam, some of the electrons of the atoms in the matter under the beam will first be energized to higher orbital positions and then drop down to their appropriate energy level again during which X-rays are emitted. The emitted X-rays are characteristic for each element and have specific energetic wavelengths and energy patterns. Therefore an elemental composition can be quantified by analyzing the energy spectrum and intensities of the X-rays emitted during the analysis.

EDS is mostly possible for Na and heavier elements. Lighter elements from Be and up may also be quantified depending detectors and instrumental configuration. Oxygen is normally not analysed by SEM EDS, but may be calculated by difference or by converting all elements to oxides. When calculated by difference, as done in this work, the sum of all elements adds up to 100 wt%.

Measurements may be made as semiquantitative or quantitative analyses using either standardless/internal instrument standard values or calibrated concentration-intensity curves using a range of relevant metals, minerals and glass standards, respectively. In the present analysis, elements were reported as semi-quantitative results. Due to current quality of detectors and in-build standard references, such results are relatively reliable for major elements if the materials have sufficiently high thickness and low roughness.

Samples were prepared by pelletizing a known amount of powder. The results are given in wt.% and parts per million (ppm) depending on the absolute concentrations in the sample materials. All TiO2 SAS materials were analyzed, but only the CNTs NM400, NM401 and NM402 were available at the time of analyses.

## 5.1.2 ICP-MS analysis

Two contributing partners (LNE and Duke University) conducted ICP-MS analyses of the MWCNT in NANOGENOTOX. LNE specifically focused on identifying a suitable extraction procedure for three different CNTs (NM400, NM401 and NM402) available at the beginning of the project followed by elemental screening of three samples. Duke University offered data from a full multi-elemental analysis on all the CNT using their in-house standard extraction procedure.

**Procedure at LNE**

LNE performed semiquantitative analysis on a quadripolar PQ Excell VG elemental ICP/MS in the standard condition

Panoramic spectra on each sample were performed in order to detect the majority elementary components and traces. An evaluation of their contents is then realized with synthetic standard solutions and blanks of acids used for the digestion of CNT samples

On the basis of work on the CNT of Ge et al. (2008), the mineralization in the microwave and closed system were attempted by varying the samples mass and the mixtures of acids for each sample. The specific extraction conditions for the three MWCNT are listed in Tables 5-1 to 5-3.

*Table 5-1. Extraction procedure for NM400*

| NM400 - Sample 0389 | | |
|---|---|---|
| 10 mg | 10 mg | 20 mg |
| 9mL HCl suprapur + 3mL $HNO_3$ suprapur | 7mL $HNO_3$ suprapur + 1ml $H_2O_2$ suprapur | 12mL $HNO_3$ suprapur + 1mL $H_2O_2$ suprapur |
| intact particles | Mineralization dissolution completed OK | Mineralization dissolution completed OK |

*Table 5-2. Extraction procedure for NM401*

| NM401 - Sample 0040 | | | |
|---|---|---|---|
| 5 mg | 10 mg | 5 mg | 7 mg |
| 9mL HCl suprapur + 3mL $HNO_3$ suprapur | 7mL $HNO_3$ suprapur + 1ml $H_2O_2$ suprapur | 12mL $HNO_3$ suprapur + 1mL $H_2O_2$ suprapur | 3mL $H_2SO_4$ suprapur + 3mL $HNO_3$ suprapur |
| intact particles | intact particles | intact particles | mineralization dissolution completed OK |

It is observed that the aqua regia (HCl + $HNO_3$) do not allow to dissolve carbon. For samples 0389 (NM400) and 0395 (NM402), the combination of $H_2O_2$ and $HNO_3$ provides a total mineralization of these particles. However, this did not work for sample 0040 (NM401), where a mixture of $HNO_3$ and $H_2SO_4$ appeared to be effective. It should be noted that efficient extraction requires a high acid volume to sample mass ratio.

*Table 5-3. Extraction procedure for NM402*

| NM402 - Sample 0395 | | |
|---|---|---|
| 10 mg | 10 mg | 20 mg |
| 9mL HCl suprapur + 3mL HNO$_3$ suprapur | 7mL HNO$_3$ suprapur + 1ml H$_2$O$_2$ suprapur | 12mL HNO$_3$ suprapur + 1mL H$_2$O$_2$ suprapur |
| intact particles | Mineralization dissolution completed OK | mineralization dissolution completed OK |

The program of mineralization used (up to 6 simultaneous mineralization) is given in table 5-4.

*Table 5-4. Mineralization program used in the sample preparation procedure*

| 10 min | 250 W |
|---|---|
| 5 min | 0 W |
| 10 min | 500 W |
| 5 min | 0 W |
| 10 min | 650 W |
| 5 min | 0 W |
| 10 min | 850 W |
| 5 min | 0W |
| Vent 5 min | |

**Procedure used by Duke University**

Multi-element metal analysis of CNT sample extracts was performed on an Agilent Technologies 7700 Series ICP-MS with an ASX-500 Series ICP-MS Autosampler (Agilent Technologies, Santa Clara, CA, USA). External calibration curve solutions (five points) were run before the samples. Additional calibration curve solutions and blanks were run as unknowns before and after sample sets to confirm calibration and determine any background contamination. The calibration curves for each metal displayed good linearity ($r^2 \geq 0.999$). Metal concentrations were calculated using these external calibration curves.

To overcome the challenges in chemical digestion of the carbon "skeleton", the CNT samples were weighed into ceramic crucibles (approximately 20-30 mg) and calcinated (or combusted) for 12 hours at 750 °C. Once cooled, 375 µL concentrated HNO$_3$ and 75 µL concentrated HCl were added to the combusted CNTs. Samples were transferred to 40 mL metal-free glass vials and heated for 1 hour at 100 °C on a heating block. Once ready for analysis, samples were transferred to 15 mL sterile, acid-washed polypropylene centrifuge tubes (VWR, Radnor, PA, USA) and diluted to 15 mL with de-ionized water for a final concentration of 2% HNO$_3$ and 0.5% HCl.

## 5.1.3 ICP-OES analysis

CODA CERVA offered elemental analysis by inductively coupled plasma-optical emission spectrometry (Varian 720-ES, Agilent Technologies), using the SemiQuant feature, which is designed to provide a fast estimate of the concentration of non-calibrated compounds in samples. The samples were screened for 68 elements (Figure 5-1) (Ag, Al, As, Au, B, Ba, Be, Bi, Ca, Cd, Ce, Co, Cr, Cu, Dy, Er, Eu, Fe, Ga, Gd, Ge, Hf, Hg, Ho, In, Ir, K, La, Li, Lu, Mg, Mn, Mo, Na, Nb, Nd, Ni, P, Pb, Pd, Pr, Pt, Rb, Re, Rh, Ru, S, Sb, Sc, Se, Si, Sm, Sn, Sr, Ta, Tb, Te, Th, Ti, Tl, Tm, U, V, W, Y, Yb, Zn, Zr).



*Figure 5-1 Periodic table of the elements showing the 68 elements that could be analysed in blue.*

To bring the $TiO_2$ and SAS NM in solution, 0.1 g was weighed in a 50 ml DigiPREP HT tube (SCP SCIENCE) for each sample and 2 ml of concentrated HF was added. The mixture was heated overnight at 80°C in a DigiPREP MS (SCP SCIENCE). After cooling, the volume was made up to 10 ml with double distilled water. A few samples (0047, 1252, 0505, 0074, 0239, 0244) was tested for the ability to dissolve the materials without heating. For these samples 0.05 g was weighed in a 50 ml DigiPREP HT tube (SCP SCIENCE). To this 2 ml of concentrated HF was added. The mixture was left overnight at room temperature, after which it was made up to 10 ml with double distilled water.

For MWCNT, the samples were calcinated. Approximately 10 mg MWCNT was weighed into a platinum crucible for each sample. The crucibles were placed in a muffle furnace after which the temperature was progressively increased up to 650°C in 12 hours. This temperature was maintained for 6 hours. After cooling, the ashes were dissolved in 1 ml $HNO_3$. Next, a few ml double distilled water were added and heated until the boiling point was reached. The remaining solution was made up until 10 ml with double distilled water. This solution was screened for semiquantitative analysis. In second instance, because of their relatively high levels and their possible toxicity, Al, Co and Fe were analyzed by quantitative ICP-OES.

## 5.2 Results

### 5.2.1 EDS analysis on powder pellets

Tables 5-5 to 5-6 list the results from EDS analyses of the pelletized powders. Minor and trace elements were given in ppm to enable direct comparison with results reported for the ICP analysis.

**$TiO_2$ NM**

NM102 and NM105 are relatively pure with presence of less than 1000 ppm Si. NM100 contains 2100 to 4900 ppm Fe, as well as Si, K and P as well as Al and trace of Cr making 0.86 wt% of the sample. NM101 contains comparable amounts of Si, Al and P as found in NM100, but also 2500 ppm S. NM103 and NM104 contained 3.2 – 3.4 wt% Al and trace amounts of Si and S.

*Table 5-5 Elemental concentrations by EDS measurements on $TiO_2$ performed at IMC-BAS.*

| Sample | Al* | Si* | P* | S* | K* | Ti (wt%) | Cr* | Fe* | O wt% |
|--------|-----|-----|-----|-----|-----|----------|-----|------|-------|
| NM100 | 900 | 2800 | 2100 | | 2500 | 58.57 | 300 | 4900 | 40.08 |
| NM101 | 900 | 2900 | 2700 | 2200 | | 58.79 | | | 40.35 |
| NM102 | 500 | 800 | | | | 59.73 | | 700 | 40.07 |
| NM103 | 34300 | 6800 | | 2600 | | 54.74 | | 600 | 40.82 |
| NM104 | 32200 | 1800 | | 3200 | | 55.60 | | | 40.68 |
| NM105 | 400 | 700 | | | | 59.81 | | | 40.07 |

\* ppm by weight

**SAS**

Table 5-6 list the elemental composition determined on the SAS nanomaterials. All samples only contain minor elemental impurities. Na makes 1800 ppm to 0.9 wt% (NM200, NM201 and NM204), whereas Al makes ca. 0.5 to 0.7 wt% (all samples) and S makes 400 ppm to 0.9 wt% (all samples except NM202). Ca was only observed in NM203 (1800 ppm). Hence, the presence of calc-alkali elements, S and Al support the analyses with occasional observation of Na sulfate and boehmite.

*Table 5-6 Elemental concentrations by EDS measurements on SAS performed at IMC-BAS.*

| Sample | Na* | Al* | Si (wt.%) | S* | Ca* | O (wt.%) |
|--------|-----|-----|-----------|-----|-----|----------|
| NM200 | 8800 | 4600 | 44.77 | 8700 | | 53.02 |
| NM201 | 4400 | 7400 | 45.27 | 4600 | | 53.08 |
| NM202 | | 4500 | 46.23 | | 1800 | 53.14 |
| NM203 | | 4300 | 46.32 | 400 | | 53.21 |
| NM204 | 1800 | 4800 | 45.96 | 2100 | | 53.17 |

\* ppm by weight

**MWCNT**

Tabel 5-7 lists the concentrations of the detected elements in the MWCNT samples. NM401 was found to contain minor impurities dominated by Cu (0.2 wt%) and Zn (0.2 wt%). Similar Cu and Zn levels were found in NM400, whereas only traces of Cu was observed in NM402. The major impurities in NM400 and NM401 is Al and Fe, where Al makes several percent in both samples as well as Fe in NM402.

*Table 5-7 Elemental concentrations by EDS measurements on MWCNTs performed at IMC-BAS.*

| Sample | C (wt%) | Al* | Si* | Fe* | Co* | Cu* | Zn* | O (wt%) |
|--------|---------|------|-----|-------|------|------|------|---------|
| NM400 | 89.81 | 46100 | 400 | 7600 | 2500 | 2000 | 1900 | 4.15 |
| NM401 | 99.19 | | 500 | | | 2300 | 2200 | 0.6 |
| NM402 | 92.97 | 21100 | 500 | 29800 | | 400 | | 1.93 |

* ppm by weight

## 5.2.2 ICP-OES analysis

**TiO$_2$ NM**

Tables 5-8 and 5-9 show the elemental concentration ranges found after screening the TiO$_2$ samples by ICP-OES. No elements in NM102 and NM105 were found to be present in concentrations higher than 0.1 wt%. Only K was found in concentrations between 0.1 and 1 wt% in NM100. Na, P, Ca, and Zr were found in trace amounts. Notably trace amounts of Zr were found in all samples, but NM105. The most anundant impurities (> 1 wt%) were found to be Al in NM103 and NM104. Na and K (both 0.1–1 wt%) were the most abundant impurities in NM102 and NM100, respectively.

*Table 5-8. Graphical summary table with the impurity ranges found in titanium dioxide.*

*Table 5-9. Overview of impurities detected in titanium dioxide NM.*

| Nanomaterial | Vial ID n° | Impurities > 0.01% | Impurities 0.005 – 0.01% | Impurities 0.001 – 0.005% |
|---|---|---|---|---|
| NM-100 | 0047 | K (>0.1%), P | Zr | Ca, Na |
| NM-101 | 1252 | Al, Na (>0.1%), P, S, Zr$^\$$ | - | K, Ca |
|  | 1265 | Al, Na (>0.1%), P, S | K, Zr$^\$$ | Ca |
| NM-102 | 0054 & 0060 | S | Ca, Zr | K, Na, P, W |
| NM-103 | 0584 & 0585 | Al (>1%), Na, S | Ca | Fe, K, Mg, Zr |
| NM-104 | 0502 & 0505 | Al (>1%), Ca, Na, S | - | K, Mg, Zr |
| NM-105 | 2209 & 2217 | - | - | Na |

$^\$$ Near 0.01%

**Synthetic Amorphous Silica**

**Erreur ! Source du renvoi introuvable.**Table 5 11 represent the major impurities found in the silica nanomaterials: Na (> 0.1% in NM-200, NM-201 and NM-204), S (> 0.1% in NM-200) and Al (> 0.1% in NM 201). Calcium was found at > 0.01% in NM-200 and NM-201. Sulphur was found at >0.01% in NM-201 and NM-204. Smaller amounts of Fe, K, Zr and Mg were found in NM-200, NM-201 and NM-204. NM-202 and NM-203 contained no detectable impurities, except NM-203:0244 where almost 0.01% of Na was found while in NM-203:0239 was not detectable

*Table 5-10. Graphical summary table with the impurity ranges found in synthetic amorphous silica.*
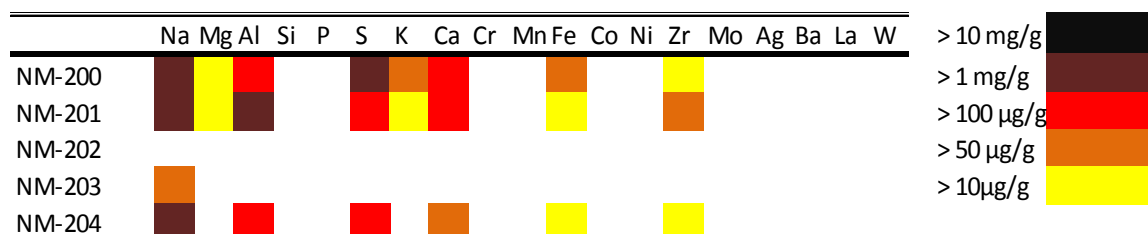


*Table 5-11. Overview of the impurities detected in SAS by semi-quantitative ICP-OES.*

| Nanomaterial | Vial ID n° | Impurities > 0.01% | Impurities 0.005 – 0.01% | Impurities 0.001 – 0.005% |
|---|---|---|---|---|
| NM-200 | 0121 & 0138 | Al, Ca, Na (>0.1%), S (>0.1%) | Fe, K | Mg, Zr |
| NM-201 | 0074 & 0079 | Al (>0.1%), Ca, Na (>0.1%), S | Zr | Fe, K, Mg |
| NM-202 | 0075 & 0102 | - | - | - |
| NM-203 | 0239 & 0244 | - | Na (0244) | - |
| NM-204 | 0079 & 0086 | Al, Na (>0.1%), S | Ca | Fe, Zr |

$^\$$ Near 0.01%

**MWCNT**

Table 5-12 and Table 5-13 represent the impurities found in the MWCNT by ICP-OES. The major impurities found were aluminium (Al; > 0.1% in NM-400 and NM-402) and iron (Fe; >0.01% in NM-400, NM-402 and NRCWE-007).

Sodium (Na) was found at > 0.01% in NM-400. Cobalt (Co), magnesium (Mg) and manganese (Mn) were found at > 0.01% in NM-403. Calcium (Ca), lanthanum (La) and nickel (Ni) were found at > 0.01% in NRCWE-007.

In NM-400 smaller amounts (≤0.01%) of Co, Ca and K were found. In NRCWE-007 a range of elements was found in amounts between 0.001 and 0.01% (Mg, Ba, Mo, Ag, Al, Co, Si, S). In sample 0013 of NRCWE chromium (Cr) was found just above 0.01% while in sample 0016 it was found just below 0.01%.

A trace of silver (< 0.005%) was found in sample 0090 (NM-401), but not at all in sample 0101. It is therefore not clear whether this is an artifact or not. Similarly, Ca was found in sample 01060 of NM-403 (> 0.01%) but not in the other samples of NM-403.

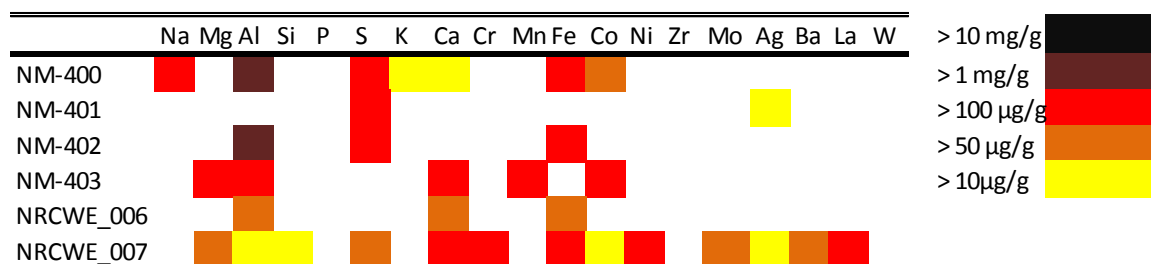*Table 5-12. Graphical summary table with the impurity ranges found in MWCNT NM.*



*Table 5-13. Overview of the impurities detected in MWCNT by semi-quantitative ICP-OES.*

| Nanomaterial | Sample ID n° | Impurities > 100 ppm | Impurities 50 – 100 ppm | Impurities 10 – 50 ppm |
|---|---|---|---|---|
| NM-400 | 0423 & 0445 | Al, Fe, Na, S[$] | Co | Ca, K |
| NM-401 | 0090 & 0101 | S[$] | -[†] | Ag |
| NM-402 | 0429 & 0431 | Al, Fe, S[$] | - | - |
| NM-403 | 1037 & 1064 1060 & 1062 | Al, Co, Mg, Mn, Ca (01060) | - | - |
| NRCWE-006 | 014 016 | - | Ca, Fe Al | - Fe |
| NRCWE-007 | 013 & 014 | Ca, Fe, La, Ni, Cr (0013) | Mg, Ba (0013), Cr (0014), Mo,S (0014)[$] | Ag, Al, Co, Si, S (0013)[$], Ba (0014), Mo (0014) |

[$] Impurity content might be higher for sulphur

To be enable assessment of the possible toxicicological role of Al, Co and Fe in more detail, these elements were subsequently analysed by quantitative ICP-OES (Table 5-14).

## 5.2.3 ICP-MS analysis

Table 5-15 lists the analytical results from the ICP-MS analysis of CNT from Duke University and LNE. NM400, NM402 and NM403 were found to be the most impure CNTs (1 and 3 wt.%). As observed by EDS, Al and Fe are the most important impurities. However, Mg (2231 ppm), Mn (2706 ppm), and Co (2881 ppm) are also important elements in NM403, whereas Ni (4800 ppm) was found to be one of the most abundant impurities in NRCWE007. The ICP-MS results indicate that Mn and Ni should also be considered as important elements for (geno)toxicity testing.

Comparing, the absolute results obtained by the two ICP-MS and the ICP-OES procedures, we find some inconsistencies: Higher concentrations of Al, Fe, and Co are generally found by the two quantitative ICP-MS analyses as compared to the quantitative ICP-OES analyses. Overall the ratios may vary by a factor up to 25 (Al) between the lowest and highest concentrations found.

*Table 5-14. Overview of the aluminium (Al), iron (Fe) and cobalt (Co) concentrations in MWCNT after calcination and analysis by ICP-OES.*

| Nanomaterial | Sample vial | Al (mg/kg) | Fe (mg/kg) | Co (mg/kg) |
|---|---|---|---|---|
| NM-400 | 0423 | 2550 | 404 | 164 |
|  | 0445 | 2530 | 369 | 158 |
| **Average ± SD** |  | **2540±14** | **387±25** | **161±4** |
| NM-402 | 0429 | 2050 | 1310 | n.d. |
|  | 0431 | 2000 | 1200 | n.d. |
| **Average ± SD** |  | **2025±35** | **1255±78** | **n.d.** |
| NM-403 | 01037 | 521 | n.d. | 518 |
|  | 01064 | 380 | n.d. | 607 |
|  | 01060 | 397 | n.d. | 629 |
|  | 01062 | 424 | n.d. | 700 |
| **Average ± SD** |  | **431±63** | **n.d.** | **614±75** |
| NRCWE-006 | 0014 | <10 | 20 | n.d. |
|  | 0016 | <10 | 28 | n.d. |
| **Average ± SD** |  | **<10** | **24±4** | **n.d.** |
| NRCWE-007 | 0013 | 25 | 397 | 39 |
|  | 0014 | 38 | 447 | 41 |
| **Average ± SD** |  | **32±9** | **422±35** | **40±1** |

n.d.: not determined

## 5.3 Discussion

EDS and ICP-OES were used to perform a semi-quantitative screening of contaminant elements in all of the NM samples. Several impurities were found in NM samples, but there was not always a good agreement between the elements reported and their concentrations. This may in part, but not always, explained by the much lower detection limit of ICP-OES and interference between specific energies in the EDS spectra obtained, which are not easily resolved in semiquantitative analysis. Examples of differences between the elemental screening results as well as the quantitative analysis of the CNT are discussed below

All $TiO_2$ samples contained trace to minor amounts (0.01 to 0.1 wt% in NM101) of Na, but Na was not detected in the EDS analyses of $TiO_2$. Similarly, Zr (from 10-50 ppm to > 0.1 wt%) was found in all

50

samples, but NM105, by ICO-OES and not identified by EDS. Opposite by EDS, Fe was found in NM100 (0.5 wt%), NM102 (700 ppm) and NM103 (600 ppm), but only detected in trace amounts in NM103 (10-50 ppm) by ICP-OES. Both types of analyses, however, identified Al and S being among the most abundant impurities in NM101, NM103 and NM104, but the relatively abundant Si impurity found by EDS was not reported in the ICP-OES analysis for these samples. In fact, Si was not detected in $TiO_2$ by ICP-OES.

*Table 5-15. Results from the ICP-MS analysis at Duke University and LNE and ICP-OES by CODA CERVA (CODA) at specified elements.*

| | NM400 | NM401 | NM402 | NM403 | NRCWE006 | NRCWE007 |
|---|---|---|---|---|---|---|
| Na | 1345 ± 151 | 581 ± 32 | 727 ± 120 | 893 ± 443 | 499 ± 103 | 505 ± 190 |
| Na (LNE) | 600 | - | - | NA | NA | NA |
| Mg | - | 0 ± 3 | - | 2231 ± 144 | 0 ± 1 | 54 ± 16 |
| Al | 9951 ± 331 | 59 ± 4 | 12955 ± 1530 | 2024 ± 168 | 66 ± 19 | 86 ± 24 |
| Al (CODA) | 2540 ± 14 | NA | 2025 ± 35 | 431 ± 63 | <10 | 32 ± 9 |
| K | 97 ± 3 | 57 ± 9 | 85 ± 7 | 88 ± 40 | 56 ± 11 | 56 ± 17 |
| Ca | 3 ± 2 | 2 ± 1 | 2 ± 1 | 2 ± 1 | 2 ± 1 | 10 ± 4 |
| V | 0 | 1 ± 0 | 1 ± 0 | 0 | 1 ± 0 | 2 ± 0 |
| Cr | 9 ± 1 | 3 ± 1 | 13 ± 1 | 3 ± 1 | 3 ± 0 | 149 ± 13 |
| Cr (LNE) | 14 | - | 10 | NA | NA | NA |
| Mn | - | - | 9 ± 1 | 2706 ± 182 | - | 14 ± 2 |
| Mn (LNE) | 2 | - | 17 | NA | NA | NA |
| Fe | 1988 ± 26 | 379 ± 71 | 16321 ± 664 | 7 ± 4 | 355 ± 2 | 480 ± 13 |
| Fe (LNE) | 4300 | NA | 16000 | NA | NA | NA |
| Fe (CODA) | 387 ± 25 | NA | 1255 ±78 | - | 24 ± 4 | 422 ± 35 |
| Co | 693 ± 26 | - | 2 ± 0 | 2881 ± 190 | - | 116 ± 21 |
| Co (LNE) | 3700 | - | 5 | NA | NA | NA |
| Co (CODA) | 161 ± 4 | NA | - | 614 ± 75 | - | 40 ± 1 |
| Ni | 4 ± 0 | 2 ± 0 | 9 ± 1 | 58 ± 4 | 1 ± 0 | 4843 ± 289 |
| Ni (LNE) | 17 | - | 11 | NA | NA | NA |
| Cu | 3 ± 0 | 3 ± 3 | 4 ± 1 | 1 ± 0 | 0 | 13 ± 0 |
| Cu (LNE) | 1 | - | 4 | NA | NA | NA |
| Zn | 2 ± 0 | 2 ± 1 | 2 ± 0 | 5 ± 1 | 1 ± 0 | 3 ± 1 |
| Zn (LNE) | - | - | 1 | NA | NA | NA |
| As | - | - | - | - | - | - |
| As (LNE) | 5 | - | - | NA | NA | NA |
| Sr | - | - | - | - | - | 1 ± 0 |
| Mo | - | - | - | - | - | 48 ± 6 |
| Mo (LNE) | 1 | - | 1 | NA | NA | |
| Ag | - | - | - | - | - | 1 ± 0 |
| Ag (LNE) | 0.3 | - | 0.3 | NA | NA | |
| Sn | NA | NA | NA | NA | NA | NA |
| Sn (LNE) | 0.5 | - | 0.5 | NA | NA | NA |
| Ba | 1 ± 0 | 1 ± 0 | 1 ± 0 | 1 ± 1 | 1 ± 0 | 64 ± 1 |
| Ba (LNE) | 0.3 | - | 0.3 | NA | NA | NA |
| Pb | 1 ± 0 | - | - | - | - | 1 ± 0 |
| Pb (LNE) | 1.5 | - | 1.2 | NA | NA | NA |
| La (LNE) | - | - | 0.1 | NA | NA | NA |
| Ce (LNE) | - | - | 0.3 | NA | NA | NA |
| Wt% | 1.41 | 0.11 | 3.01 | 1.09 | 0.10 | 0.64 |
| Wt% (LNE) | 0.87 | - | 1.6 | NA | NA | NA |

NA: Not analyzed or Not reported; - Not detected.

In the analysis of the SAS NM, the trace impurities found EDS were Na, S and Al, as well as Ca instead of Na in NM202. The EDS data are in good agreement with the main trace impurities observed by ICP-OES, where lower ppm-range concentrations of Mg, Fe, and Zr were also observed. Hence, the inorganic chemical analyses correspond well to the observations of $Na_2SO_4$ and boehmite by XRD.

The analyses of the CNT NM showed clearly different elemental profiles of the different CNTs suggesting that they were produced using different catalysts. However, the results were relatively inconsistent; both regarding which elements that were detected and their concentrations. The differences in elemental profiles is naturally, in part, caused by the different detection limits of the two methods, where SEM EDS becomes questionable around 0.01 wt% and ICP MS and ICP-OES have detection limits in the ppm and ppt range, respectively. However, presence of un-detected elements and the very different concentration levels obtained for same elements is of concern.

First, there were large differences between the EDS and ICP-OES data obtained in the screening analysis. By ICP-OES relatively high impurity concentrations were only observed in NM400 and NM402 and dominated by Al (>1 wt%). The relatively high Al concentrations in these two NMs are in agreement with the results from the EDS analyses. All other elements determined by ICP-OES were in concentrations lower than 0.01 wt%. This is in contrast to the EDS analyses (NM400, NM401 and NM402) Fe, Co, Cu, and Zn may also be present in concentrations higher than 0.01 wt%. Specifically, the Fe concentration was found to be 7600 and 29800 ppm in NM400 and NM402, respectively.

Second, unfortunately all CNT samples were not analyzed fully by quantitative procedures and some CNT were not analyzed by all methods. This makes a complete comparison difficult. However, when possible, for comparison, it appears that there is reasonable consistency in the detected elements, but not necessarily in the concentrations determined.

Comparing the results for some of the key catalyst impurities, Al, Fe, and Co, shows interesting linear relations between the different data series (Figure 5.1). It is evident that the ratios between the analyses vary depending on the procedures used. Lowest concentrations were obtained by the procedure used by CODA-CERVA followed by the procedures used by Duke University (ICP-MS), LNE (ICP-MS), and IMC-BAS (EDS). It is anticipated that the explanation for these more or less systematic differences is caused by the different digestion procedures used rather than instrumental settings and qualities. This is further supported by the fact that the highest concentrations were generally obtained by EDS, which is a non destructive method.

Comparing the elemental analyses of the CNT samples with the results of the TGA-analysis further support this hypothesis. Table 5-16 list the total elemental concentrations reported for each of the analyses and the total incombustible residual from the TGA analyses. In some cases, the elemental analyses still remain to explain several weight percent inorganic elements.

Overall from the elemental analyses, it must be concluded that further work remains to be done in development of elemental analysis for certain NM. In this case, inconsistencies were observed for CNT, but also $TiO_2$ NM. For ICP analyses, extraction procedures should be further evaluated. Additionally, analytical methods such as XRF and INAA should be considered to avoid the challenges in digestion of complex materials with great variation in elemental concentrations.

Co-funded by
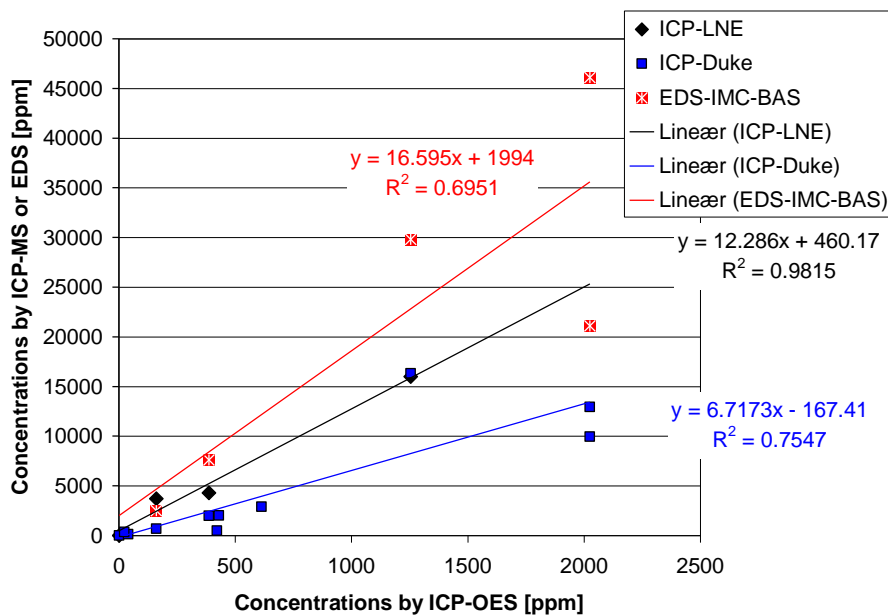the Health Programme
of the European Union

Figure 5-1. Plot of elemental concentrations of selected catalyst impurities in CNT determined by quantitative ICP-MS and semiquantitative EDS plotted against results from quantitative ICP-OES analysis.

*Table 5-16. Overview of the aluminium (Al), iron (Fe) and cobalt (Co) concentrations in MWCNT after Total impurity and catalyst amount quantified by the different listed techniques*

|                     | NM400 | NM401 | NM402 | NM403 | NRCWE006 | NRCWE007 |
|---------------------|-------|-------|-------|-------|----------|----------|
| EDS metals          | 6.05  | 0.5   | 5.18  |       |          |          |
| ICP-MS-Duke         | 1.41  | 0.11  | 3.01  | 1.09  | 0.1      | 0.64     |
| ICP MS-LNE          | 0.87  | -     | 1.6   |       |          |          |
| ICP-OES-CODA CERVA  | 0.31  | -     | 0.33  | 0.10  | <0.01    | 0.05     |
| EDS incl Oxygen     | 10.2  | 1.1   | 7.11  |       |          |          |
| TGA                 | 16.2  | 18.1  | 10.6  | 3.2   | 17.6     | 6.2      |

# 6 Analysis of associated organic matter

## 6.1 Analytical procedure

The results from the TGA analyses were used to identify NM which potentially could be coated or associated with organic compounds. In the current analyses, a threshold value of 1 wt% weight-loss above 110°C was used. In this case, these NM include NM101, NM103, NM104 and NM204.

After NM selection, the organic compounds were either extracted using ASE (Accelerated Solvent Extraction) or desorbed by TD (Thermal Desorption). The solvent extraction can be used for several chromatographic and mass spectrometric techniques and enable quantitative determination, but it has been found that TD combined with gas chromatography – mass spectrometry (GC-MS) generally is suitable for screening of the samples for up to intermediate molecular weights of the organic coatings. However, for each NM, the thermal stability and the solubility of the coating must be considered before extraction or desorption. If for example the organic coating material consists of high molecular weight component MALDI-TOF-MS (Matrix Assisted Laser Desorption Ionization – Time Of Flight) or ESI-MS (Electrospray Ionization) would be good choices instead of GC-MS.

In this case, approximately 300 mg of each NM with potential organic coating was methanol extracted using ASE and analyzed using on-column GC-MS.

The extract was injected directly (1 μl) into the on-column-GC-MS which was equipped with a FactorFour™ 30 m VF-5ms capillary column with a diameter of 0.25 mm and 0.25 μm stationary phase containing 5 % phenyl poly dimethylsiloxane (Varian). The column flow was 1 ml/min helium and the injector temperature at 50°C was held for 2 min and then heated to 250°C at a rate of 50°C/min. The GC oven program was 50° for 4 min increased by 4°/min to 120° and 8°/min to 250° and held for 10 min. The transfer-line temperature was 275 °C. The MS was run in positive mode using EI (electron ionization). Scanning mass range was from 50 to 500 m/z. Identification of the organic compounds was performed by AMDIS version 2.65 June 26, 2008 and NIST/EPA/NIH Mass Spectral Library Version 2.0f, 23 June 25, 2008 (NIST, USA). Compounds for which authentic standards were used and matched both retention time and spectrum were considered as clearly identified. The following GC-MS properties of the authentic standards were used for identification: Retention time ($t_R$), mass spectrum (MS spectrum), fragmentation pattern and peak shape.

## 6.2 Results

Based on the TGA results, apparent presence of organic coating was identified for NM-101, NM-103, NM-104, and NM-204. The results from the GC-MS analysis at NRCWE are listed in Table 9-3. Compounds assigned a succeeding question mark (?) are considered as tentatively identified. As can be seen, the organic compounds appear to generally consist of silanes. Glycerol was found in NM104 only.

Tetramethyl silicate was found in three out of the four samples. The content of tetramethyl silicate in the extracts was surprising due to its relative high chemical reactivity (hydrolysis). However, indirect proof of the presence in the extracts was the observation that the peaks of tetramethyl silicate disappeared few days after extraction. This was also the case for the authentic tetramethyl silicate standards. Water vapour from the laboratory air will undoubtedly be taken up by the extracts and

55

standard solutions and degrade tetramethyl silicate by hydrolysis. Tetramethyl silicate in the extract of $SiO_2$ may be a residue from production which may have been based on synthesis from tetramethyl silicate. Alternatively, tetramethyl silicate may have been produced during the extraction process which uses relatively harsh extraction conditions (150 °C and 140 bar) and methanol, either directly through reaction of $SiO_2$ with methanol or from tetraalkoxy silanes with other chain lengths in the samples, which in excess alcohol and basic conditions may produce tetramethyl silicate. So far we have not been able to confirm or disconfirm these hypythesis. GC-MS analysis of other samples, where coatings were indicated by TGA, did not reveal presence of any organic coatings.

*Table 5-1. Results from the GC-MS measurements at NRCWE. The apparent relative abundance is estimated from low (x), intermediate (xx) to high (xxx).*

| Compounds in the order of retention time On-column-GC-MS | Retention time (min) | Nanogenotox | | | |
|---|---|---|---|---|---|
| | | NM-101 | NM-103 | NM-104 | NM-204 |
| | | $TiO_2$ | $TiO_2$ | $TiO_2$ | $SiO_2$ |
| Dimethoxydimethylsilane | 2.4 | | xxx | | |
| Silane? | 3.3 | | x | | |
| Tetramethyl silicate€ | 4.9 | | | xx | xxx |
| Silane? | 7 | | xx | | |
| Glycerol? | 13 | | | xx | |
| Silane? | 31.6 | x | | x | |
| Silane? | 32.9 | x | | x | |
| Hexadecanoic acid, methyl ester | 33.4 | xx | | xx | x |
| Hexadecanoic acid | 33.9 | x | | x | x |
| Octadecanoic acid, methyl ester | 35.8 | xx | | xx | x |

€ uncertain identification

# 7 Conclusions

XRD analysis is known to be an excellent tool for identification of the crystalline form of crystalline materials. The results in this study showed general good agreement between the results from the three participating laboratories. However, there may be differences, as documented for e.g., SAS, which may be attributed to different instrumental configurations and performances. The type of sample mount and amount may also play a role on the ability of detection. XRD analyses on CNT did not reveal clear usability for analyzing and characterizing XRD by this method.

XRD may also be used for quantitative assessment of the average crystallite size of crystalline materials. For this many different programs may be used to calculate the sizes using either direct peak broadening or analyses after refinement of the XRD profile. Major effort was set to compare the calculated values of the crystallite sizes for the samples using a range of different methods. The results showed high inconsistency when the crystallite size was larger than 100 nm, where quantification of size is doubtful. NRCWE generally found coarser crystals using the same material for investigation.

TGA and DTA were found to be very useful for identification of samples which may be coated or associated with organic compounds. In addition, TGA showed that sufficient sample sizes is of great concern in analyses of CNT. Most CNT products needed sample sizes higher than ca. 10 mg to be representative of the CNT products. The residual after CNT combustion in air indicated the amount of inorganic impurities (mainly residual catalyst material) that was available in their quantitative determination of the impurities.

The elemental composition of any powder or dispersed material is essential information for categorization of the substance; evaluate the potential presence of inorganic coatings, catalysts and un-intended impurities. In this work three different methods were used, including energy dispersive X-ray spectroscopy (EDS or EDX) on powder tablets and inductive coupled plasma (ICP) with mass (MS) or optical emission spectrometry (OES) for detection and quantification of extracted elements. Comparing the analyses suggest that there may be some inconsistencies in the analyses using ICP and XRF, respectively. The lag of agreement is evident for the analyzed $TiO_2$ and CNT NM. It is assumed that the observed differences may arise due to different extraction efficiencies. However, inhomogeneities may also contribute to the observed variability.

Organo-chemical analysis was made on NM101, NM103, NM104, and NM204 where the mass-loss was greater than 1 wt%. The identification of coating was expected for both NM103 and NM104, which is reported to have 2% dimethicone. Organic coating was not expected on NM101 and NM204, despite NM101 was reported to have a weight-loss of 9wt% upon calcination. Extraction followed by GC-MS analyses indicates a range of different silanes (NM101, NM102 and NM203) and glycerol (NM104). Tetramythyl silicate (with uncertain identification) may be present as coating in NM104 and NM204, however it may also be an artifact of ACE extraction. Determination of specific organic compounds used for NM functionalization and coating remains as being a challenging task.

# References

This report is based on the interim project reports and direct contributions from all co-authors. Most of the interim reports are available for the NANOGENOTOX consortium on the CIRCA web-page and not cited specifically in this report.

Ge C, Lao F, Li W, Li Y, Chen C, Qiu Y, Mao X, Li B, Chai Z, Zhao Y (2008) Quantitative Analysis of Metal Impurities in Carbon Nanotubes: Efficacy of Different Pretreatment Protocols for ICPMS Spectroscopy. Analytical Chemistry, vol. 80, no. 24, pp. 9426-9434. DOI: 10.1021/ac801469b

Jensen K, Clausen P, Birkedal R, Kembouche Y, Christiansen E, Levin M, Koponen I, Jacobsen N, Wallin H, De Temmeman P-J et al: Standard operating procedures for characterization of the selected manufactured nanomaterials and dispersions thereof. In: Standard operating procedures for characterization of the selected manufactured nanomaterials types. Edited by Jensen K, Thieret N; 2011.

Hill R.J., Madsen IC (1986) The effect of profile step width on the determination of crystal structure parameters and estimated standard deviations by X-ray Rietveld analysis. Journal of Applied Crystallography 19, 10-18. DOI: 10.1107/S0021889886090076

Langford JI, Wilson AJC (1978) Scherrer after sixty years: A survey and some new results in the determination of crystallite size. Journal of Applied Crystallography, 11, 102-113. doi:10.1107/S0021889878012844

TOPAS 4 Tutorial.pdf. Bruker AXS, no DOC-M88-EXX062 V4. Updated: Feb 27, 2008

Wojdyr M (2010) Fityk: a general-purpose peak fitting program, Journal of Applied Crystallography: vol. 43, p. 1126-1128.

# Appendix A. Standard operation procedures

## *General SOP for phase identification and determination of crystallite size using powder X-ray diffraction analysis*

**Renie Birkedal (NRCWE)**

## General description

This method is a general procedure for identification of crystalline materials in powders and calculation of average crystallite size using powder X-ray diffractometry.

The principle is that crystalline materials diffract X-rays in a characteristic pattern, which is unique for each material. XRD can therefore be used to identify different polymorphs, e.g. rutile and anatase. The width of the reflections can also give information about the size of the diffracting crystals (not necessarily the same as the particle size).

XRD can be measured in different setups and depending on the information wanted, the setup must be chosen. Different wavelengths are also possible, but for standard measurements this is less important, as long as it is remembered and taken into account. Most databases are based on irradiation using Cu X-rays. The step length (if using Cu) is recommended to be 0.15. (Hill, 1986)

Reflection data is usually chosen for a fast identification of phases. It has the advantages that very small samples can be used (though larger is recommended) and the scatter is usually to high values of 2θ, so unit cells can be determined with high accuracy.

Transmission data are better for further calculations, such as analysis and determination of atomic structure and strain, because in this case, the X-rays have passed through the whole sample.

## Materials and equipment

- Powder material
- X-ray diffractometer
- Sample holder (e.g, Al-holder, [001] quartz-holder or plastic holder)
- Glass-plate to flatten powder surface
- Data-collection software
- Data treatment software (e.g, TOPAS and Fullprof)
- 

## Sample preparation

The powder sample is placed in the sample holder. For reflection data the sample holder is usually flat, app 1.5 cm in diameter and 2 mm thick. The sample is pressed in the sample holder to ensure a

59

**www.nanogenotox.eu**

flat sample with the correct height. For transmission the sample is placed in the sample holder – usually a capillary tube, between two thin sheets of foil or on tape.

If the powder is too coarse the sample should be grinded prior to analysis to minimize preferred orientation effects. It the crystal size is to be calculated this is not an option.

Sample time depends on the detector, the X-ray tube and the sample.

## General data treatment

Identification of materials is done using databases, whereas the phase composition and crystallite size are calculated using dedicated software. Most diffraction programs can be used for calculating the ratio between phases (if the phases have been identified).

Some programs (e.g. TOPAS and Fullprof) can be used for calculating the average crystallite size. Almost all programs can also be used for refining and listing FWHM (full width at half maximum), alternatively this can be measured. FWHM can be used together with Scherrers formula to calculate an approximate average crystal size. The most accurate result is obtained, if the K-factor (the shape factor) in Scherrers formula is found by calibration with the same material as the measured.

## Comments on use and applicability

Estimation of amorphous content based on addition of material is not recommended. It is difficult to ensure an effective mixing and by adding a crystalline material one may shadow the presence of other materials or the dopant.

Results from quantitative determination of bulk phase composition (proportions) and average crystallite sizes may be affected by the settings chosen to mathematically fit the X-ray diffractograms as well as by the type of reference or standard used to obtain the diffractogram. Observations indicating these phenomena have been made in NANOGENOTOX and are currently under investigation.

# Identification and quantification of crystalline phases of TiO$_2$ powders crystallite sizes using the X'pert Pro MPD diffractometer

**Charles Motzkus (LNE)**

## General description

This procedure describes a method for identification of crystalline phases and crystallite sizes of TiO$_2$ powders using the X'pert Pro MPD diffractometer. This diffractometer has a $\theta$ - $\theta$ goniometer configuration enabling the characterizing of powders at high diffraction angles. The secondary optical focusing of X'pert Pro MPD can deliver analysis mode "skimming" for very low diffraction angles. The powders are prepared and placed in a rotating sample holder; the Spinner, which increase the bulk analysis by obtaining diffractions from a very high fraction of the material in the irradiated sample volume. Thus the value of the ratio intensity/resolution is high.

The linearity of the incident beam diffraction is regularly checked. The verification of the position of the goniometer which is performed using a single crystal of silicium allows to determine the identification of crystalline phases.

## Materials and methods

- Test material (powder)
- X-ray diffractometer Type X'pert Pro MPD
- Anode X-Ray tube Cu 50kV 35mA
- Multiple sample holders and automatic changer 15
- Primary and secondary optical focusing
- Software X'pert High Score + Stress & Texture
- Database ICDD 2009

Verifying the alignment / single crystal Si:

- Results 4 / 1000
- Value of acceptance linearity 4 / 100
- Adjustment of optimum settings of the beam by fluorescence : intensity / resolution
-

## Preparation of the samples:

The number of samples for analysis for each reference is equal to 2 in order to estimate the repeatability of the measurement.

These samples were stored at 20°C. For analysis, nano-TiO2 powders were prepared and placed in sample holders for Spinner. During the diffraction analysis, the samples were rotated in order to increase the diffraction phenomena on all the crystals in the sample. Thus, the value of the ratio resolution/intensity was high and allowed treatment of the diffractograms. The analyses were performed for two samples (two bottles) of each reference (NM).

## Measurement protocol

The diffractograms were obtained with a scan on range of 2θ from 3 to 140°. The stepping of the goniometer was fixed for these tests to 0.003° for an acquisition time of 300 s. The chamber temperature was 25°C. Analyses were performed at 50kV and 35mA.

For different spectral analysis, peak areas were preferred against intensity: the background was subtracted and only the most intense peaks without recoveries were identified.

Quantification is recommended using the "Reference Intensity Ratio (RIR)" method. The principle of this method is based on the determination of the ratio between the intensities of main peaks of each phase in relation to corundum for a mixing 50/50. The values constitute the RIR recorded for some of the phases in the ICDD database (the International Centre for Diffraction Data).

The phase identification and quantification are made with the ICCD database on the crystalline phases. This method can be considered quantitative if there are only two main phases in the $TiO_2$ powder: e.g, anatase and rutile. The number of samples for analysis for each concentration must be at least 2 to estimate the repeatability of the measurement.

We determined the association of Nickel filter, masks, slot and anti-scatter since these conditions leads to better results resolution / intensity spectrum exclusively for analysis on specifics powders. The average size of crystallites is obtained from the Scherrer equation by treatments of spectra.

## Observations on use and applicability

Preliminary internal analysis report of 6/11/2009 indicated a shift of the beam equal to 4/1000. This shift is not significant because the accepted value provided by the manufacturer is equal to 4/100.

Variability analysis of NM samples may require more than analysis of 2 different sub-samples or vials as indicated in this procedure.

## *Models used for determination of crystallite sizes by XRD*

## The Scherrer equation

The Scherrer Equation was proposed by Paul Scherrer in 1918.

$$\tau = \frac{K \cdot \lambda}{\beta \cdot cos\theta}$$

τ = the crystal size
K = Shape factor
λ = wave length
β = additional broadening (in radians) measured at half maximum.
θ = Bragg angle

The shape factor, K, depends on the crystal system and on the specific reflection (named by hkl or hikl). For cubic crystals there is only little diversity in K for different hkl, whereas for crystals with crystal symmetry has more diversity in the K value for different reflections.

As an approximation the value 0.89 or 0.9 is often used as K regardless of the reflection.

The factor for additional peak broadening, β, is calculated as $FWHM_{observed} - FWHM_{instrument}$. The contribution from the instrument is found by using a crystalline standard as shown above.

The value 0.89 has been used by NRCWE to calculate the crystal size by the Scherrer Equation. The width and position of the reflection has been found by using the program "fityk". No structure is added in this program, it is merely calculating the best fit of the peak shape.

## Winfit

The exact determination of peak parameters like area and breadths from experimental diffractograms is hindered by peak overlap and noise. Especially if Fourier or variance techniques are used for determination of crystallite size and lattice strain, the exact profile of a reflection has to be known. Small amounts of remaining noise can cause failure of the analysis. Any smoothing procedure on the other hand leads to distortion of the original peak profile. A better way is to model a Profile Shape Function (PSF) to the experimental data and calculate the variables of interest from the function parameters. WINFIT is split in two sections:

A decomposition of a complex or noisy pattern by fitting of PSFs and a XRD crystallite size section.

The **refined profiles** are used for the determination of positions (**2theta**), breadths (**FWHM)**, areas (**integrated intensity**), **crystallite size** and **lattice distortion**.

Fitting of PSF

After loading a diffractogram, the user is asked to mark an angular range for fitting and to select the peaks for refinement by mouse-clicking. From this an initial approximation of the fitting parameters are made which are refined afterwards by the Levenberg-Marquardt method (Press et al. 1992).

The PSF used is a split Pearson VII function that, if requested, can be fixed to Gaussian, Lorentzian or any intermediate type. One can choose between a unique line shape for all reflections or individual shapes for each line. Decomposition of the alpha2-component of the pattern can be selected. The satellite line is then modelled by the shape of the alpha1-line, having about half its intensity and a position calculated from that of the alpha1-peak.

WINFIT calculates the commonly used criteria for goodness of fit, e.g. the reliability or residual error (compare Howard & Preston 1989), which are a measure of the squared deviation between observed and calculated intensities. If noise is present in the original data, these criteria will indicate a "poor" fit, even if the actual peak profiles are perfectly matched. To obtain additional information on how "good" the fit matches the unknown original profile, WINFIT calculates the "absolute difference" as difference between the sums of observed and calculated data divided by the sum of observed intensities. This is graphically illustrated in Figure 3-4.
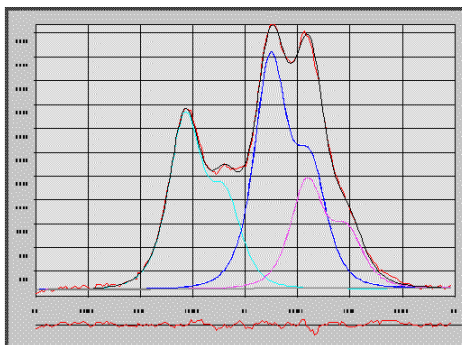
*Figure 0-1. Fitting results of a spectra and residual (error) indicated by the horizontal line below the x-axis.*

<u>Determination of crystallite size</u>

The refined peak shape parameters are used for the calculation of crystallite size and lattice strain by various single line methods and multi-order procedures. Methods based on FWHM and integral breadths are described in detail among others by Williamson & Hall (1953), Klug & Alexander (1974) and Ziegler (1981). WINFIT utilises the single line variance approach of Toth (1979) and Arkai & Toth (1983). Additionally, a procedure for separation of size and strain proposed by Dehlez et al. (1993) is available. From the Pearson exponent of the PSF the contribution of Gaussian and Lorentzian components can be calculated that are assumed to be proportional to the amount of small crystallite size broadening and strain broadening respectively. Finally, size and strain parameters are calculated by Fourier analysis. These procedures and their applicability are largely discussed in the literature (Warren & Averbach, 1950; Wagner & Aqua, 1964; Klug & Alexander, 1974; Eberl & Blum, 1993). Therefore, only the modifications and data pretreatment will be presented here.

The method proposed by Warren-Averbach makes no assumption about the form of the peak profile and the size coefficient, Enzo's method restricts the peak profile to a pseudo-Voigt function, but the size coefficient is also calculated as in the Warren-Averbach method. Balzar's method restrains the peak profile, the size and the strain coefficients to a Voigt function. Balzar's and Enzo's method separates the size and strain coefficient following Warren-Averbach. If A(L) is the Fourier transform for the intrinsic peak profile, then

$$A(L) = A^{size}(L).A^{strain}(s, L)$$

$A^{size}(L)$ is the unknown size coefficient and the strain coefficient is given by

$$A^{strain}(s, L) = \exp(-2\pi^2 s^2 L^2 <\varepsilon^2(L)>),$$

where s is the variable in reciprocal space, L is the column length of orthogonal diffracting planes and $e^2(L)$ is the mean-square strain, orthogonal to diffracting planes, averaged over the distance L.

Further, an experimental diffraction profile [h(i)] is composed of several components. The profile related to the crystalline state of the specimen [f(i)] is broadened by convolution with the profile due to machine effects [g(i)]. Additionally, a background [backgr.] due to diffuse scattering and fluorescence is present.

h(i) = (f(i) o g(i)) + backgr.

Machine dependent broadening can be removed by Fourier-methods like the Stokes correction (Stokes 1948). The deconvolution then yields the pure diffraction profile. This itself is the product of the interference function (I) and the theta dependent functions of the polarization factor (LP) and the layer structure factor (F) (Reynolds 1989).

I(i) = I(i) * LP(i) * F(i)

If a scattering domain consist of only a few layers, the variation of F and LP with angle causes an asymmetric broadening and peak displacement, due to the large angular area over which scattering occurs (Reynolds 1989). While the Stokes method corrects for instrumental errors it does not account for the LP and G functions. This is obvious from peaks that are still rather asymmetric after the Fourier-correction.

Eberl & Blum (1993) pointed out, that the Fourier method of Warren-Averbach should be applied to the pure interference function. Therefore, the effects from the other two functions (LP and F) must be removed prior to Fourier analysis.

A correction against the LP factor is easily made by division of I by LP

The procedure used for Fourier analysis:

1) Each standard and sample peak is modeled by one or more profile shape functions.

2) Then sample and standard profiles are calculated from the profile parameters obtained and are expressed in terms of the angular variable 2sin(theta)/lambda rather than in 2theta (Wagner & Aqua 1964), i.e. the calculations are performed in reciprocal space.

3) The profiles obtained are deconvoluted by the Stokes correction using a modified routine of Press et al. (1992).

4) The LP factor and the structure factor is calculated for each angular increment

5) One half of the deconvoluted profile is divided by the LP-factor and the structure factor and finally mirrored to the side were zero F-values occur.

6) This corrected profile is Fourier transformed and the coefficients [An(n)] are plotted versus the harmonic number [n]. The steepest part of this function is linearly extrapolated to An(0) and all values are renormalized to give An(0)=1. The linear extrapolation of the steepest part towards An(n)=0 yields the mean number of coherently diffracting domains.

7) The second derivative of the An(n) versus n plot gives the crystallite size distribution. The derivative is determined by a fitting a 9 point second degree polynomial (Savitzky & Golay, 1964) to the curve.

Additional features

The program does not only calculate the crystallite-size distribution and the cumulative frequency distribution, but also plots a reduced curve (Fig. 3-5). This curve is obtained by dividing crystallite size by mean crystallite size and plotting this against frequency/maximum frequency. This curve can be compared to the log normal distribution described by Eberl & Blum (1993) that is characteristic for

65

crystal growth by Ostwald ripening processes. In order to evaluate the reliability of a certain crystallite-size determination method, the program offers a function to simulate a diffraction pattern for various crystallite size distributions. The pattern is calculated from the interference function, the LP-factor and the structure factor for a "normal" quartz. No convolution of this pattern with the instrumental error functions is made. Therefore, in test runs the standard profile parameters must be set to very small breadths to yield correct values.
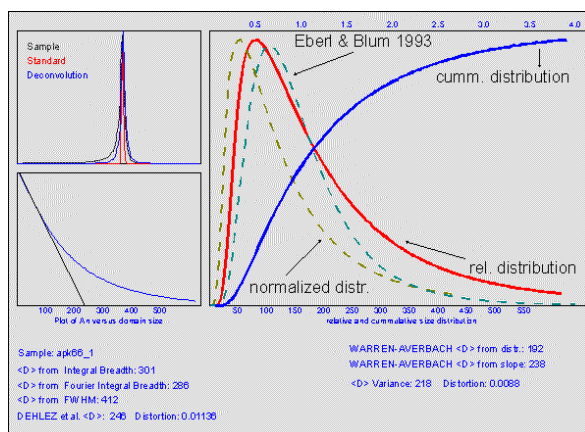


*Figure 0-2. Graph from WINFIT showing calculated crystallite-size distribution, cumulative frequency distribution, and a comparative fitting ("reduced") curve for assessment of the estimate against the theoretical Eberl and Blum Oswald ripening crystal growth curve.*

## Fullprof

The microstructural effects within FullProf are treated using the Voigt approximation: both instrumental and sample intrinsic profiles are supposed to be described approximately by a convolution of Lorentzian and Gaussian components.  The integral breadth method to obtain volume averages of sizes and stains is used to output a microstructural file where an analysis of size and strain contribution to each reflection is written.  The instrumental broadening was measured using the strain-free NIST SRM1878a standard with median grain size of 1.4 µm.

First a refinement on the standard was performed to account for the instrument contribution. The zero point displacement, background, unit cell, structural and instrumental parameters were refined. The U, V, W and X, Y instrumental FWHM parameters were placed in a separate file *.irf. Then the starting file *.pcr for each of the studied samples was modified for using the Thompson-Cox-Hastings pseudo-Voigt profile function and the instrumental parameters from the *.irf file. The zero point displacement, background, and unit cell parameters were refined (the background parameters were calculated on the base of manually extracted points).  Then size of the crystallites was refined using appropriate (according the sample symmetry) spherical harmonics SIZE MODEL.

## TOPAS

Refinement at IMC-BAS

Crystallite size was determined using the TOPAS (Bruker AXS) software. For modelling of microstructure effects TOPAS is supporting the Double-Voigt Approach, where crystallite size and strain comprise Lorentzian and Gaussian component convolutions varying in 2θ as a function of $1/\cos\theta$ (Lorentzian part, crystallite size) and $\tan\theta$ (Gaussian part, microstrain).

Calculations of sizes were done by using the whole diffraction pattern - Rietveld method.

<u>Refinement at NRCWE</u>

The NRCWE has chosen to report both the size calculated based on integral breath (IB) and full width at half maximum (FWHM).

First the starting files (*.par, and *.ins) were loaded into the TOPAS program. Then the data file for the large crystallite standard, $CeO_2$, was loaded and the structure was added into the program. All parameters were refined for the standard (zero point displacement, background, unit cell etc.) except size and strain. The peak shape was also refined, using the peak type P VII.

Refinement on the standard was done to account for the instrument contribution.

After stopping refinement on the peak shape, the data file was exchange by the data file of the sample and the structure was replaced by the structure of the sample. In the case of NM105 both the Anatase and Rutile crystal structure were loaded.

The refinement on the data included background, unit cell etc. This time size and strain were refined, whereas the peak shape was not.

# SOPs development for quantitative elemental analysis of catalyst impurities in CNTs using ICP-MS

**Charles Motzkus (LNE)**

## General description

This method has been tested to investigate its feasibility for analysis of inorganic catalysts associated with CNT.

## Materials and equipment

The data from LNE were measured on Quadripolar ICP/MS from VG Elemental, PQEcell in the standard condition.

ICP  parameters:

> - 27, 12 Mhz frequency R.F generator
> -    ICP power 1350 W

- cooling Ar flow rate : 15 l/min
- auxiliary Ar flow rate : 0,5 l/min
- nebulization Ar flow rate : 0,9 l/min
- sample uptake flow rate : 1 ml/min
- concentric glass nebuliser
- quartz torch

Quadripolar spectrometer parameters:

- interface with 1 sampler and 1 skimmer cones
- extraction lense : - 470 V
- pole bias : + 2,1 V
- focus : + 15 V
- mass spectrometer resolution : 0,7 u.m.a.
- detector autorange pulse counting / anologue mode : $10^8$ order of magnitude

## Samples pre-treatment

Under normal conditions Inductively Coupled Plasma – Mass Spectrometer (ICP/MS) works on liquid samples (Jarvis et al., 1992). Nano Carbon Tubes, NCT, have to be dissolved. Due to the very small sizes of the particles this kind of solid materials appears to be very difficult to put in solution. Some works have been done on this subject. So the LNE procedure to digest the NCTs samples will be according to the work performed by the NCNT (Chen et al., 2008).

## Impurity analysis

## External calibration of ICP/MS

For routine analysis, ICP/MS is calibrated with a linear regression curve using synthetic standard solutions of the elements to be analysed (ISO, 2007a,b). In this case accuracy of the results depends of the comparability between the sample matrix and the standard solutions. Sample matrix effect is generated in the ion source, inductived coupled plasma, by the major components present in the sample. In case of CNTs, carbon will produce this effect inducing a bias in the accuracy of typically  - 20 %  to - 30 % .To overcome this problem closed matrix matching similar to the sample can be added to the standard solutions but in case of carbon it is complicated (high purity needed). Another way is the use of a Certified Reference Material (CRM) but in the case of CNTs it doesn't exist currently.

## Standard addition method

Analysis of metals using ICP/MS can be performed with the standard addition method, internal calibration of ICP/MS. This method consists in adding in the sample several small amounts of the element of interest, typically  0,5 – 1 – 2 times of the preliminary estimated residual amount in the unknown sample. A linear regression curve can be also established and the intercept point allows

68

Co-funded by
the Health Programme
of the European Union

determining the amount of the metals in the sample. This method overcomes the matrix effect and gives in some cases good accuracy but its use is sample and time consuming.

## Isotope dilution, primary method

Isotope dilution is recognized as a primary method by the Comité Consultatif pour la Quantité de Matière (CCQM) from the Bureau International des Poids et Mesures (BIPM). This method is based on the addition of one unique amount of the element to be analysed directly in the sample. This amount has the particularity to present an artificial modified isotopic composition from the natural isotopic abundance of this element (de Bievre, 1994). This adding is called "Spike" .

By the measurement of the ratio of two selected isotopes in a blend sample-spike, the concentration of the element of interest in the sample can be directly determined. This method is very accurate for trace metals analysis, with expanded uncertainties of few percents, and free from matrix effect. It can be applied if the element of interest has more than one natural isotope, poly-isotopic, and if enriched spike for this metal is available. Isotope dilution needs a metrological approach and it is time consuming.

## Comments on use and applicability

Test analyses have shown that challenges in extraction of metal catalyst material from CNT may be substantial and cause. Alternatively, other matrix effects are in play. Therefore, standard addition or isotope dilution methods will also be considered. Another issue is sample homogeneity of CNT. The appropriate sample size may be larger than anticipated.

## *SOP for identification and analysis of organic coating*

**Per Axel Clausen (NRCWE)**

## General description

Today several NM are coated or functionalized to improve their general applicability, functionality or miscibility in matrices. Currently, there are no standard methods available proposing the pathway and analytical equipment required to identify and characterize the multitude of coatings, which is already in use. Unfortunately, there is no single analytical method that can cover analysis of all possible organic compounds used for functionalization and coating of NM. To close this gab, a procedure identification of an organic fraction and subsequent analysis is under development in NANOGENOTOX and a draft version is presented hereafter.

## Proposed procedure for identification of an organic fraction in unknown NM.

Thermogravimetry (TGA) is used to verify whether the nanomaterial (NM) is coated or not (see SOP for TGA). If the TGA analyze shows a positive response a more specific characterization will be carried out. There are number of analytical techniques which can be used, and a standardized protocol for determination of the coating is not easy to make and will be in constant development. Experience and technics in house will be very important for the choice of method. ASE (Accelerated Solvent Extraction) extraction or TD (Thermal Desorption) would be a good choice to extract the coating from the particle. A solvent extraction can be used for several analytical technics and will also give the possibility to make quantitative determination, but it is a more time consuming method. To get a quick overview of the coatings on the particles TD-GC-MS will be a good choice. For each NM the thermal stability and the solubility of the coating must be considered before extraction or desorption. The identification of the organic coating requires as many information of the NM as possible which will also determine the choice of method. If for example the coating material consists of high molecular component MALDI-TOF-MS (Matrix Assisted Laser Desorption Ionization – Time Of Flight) or ESI-MS (Electrospray Ionization) would be good choices and not GC-MS.
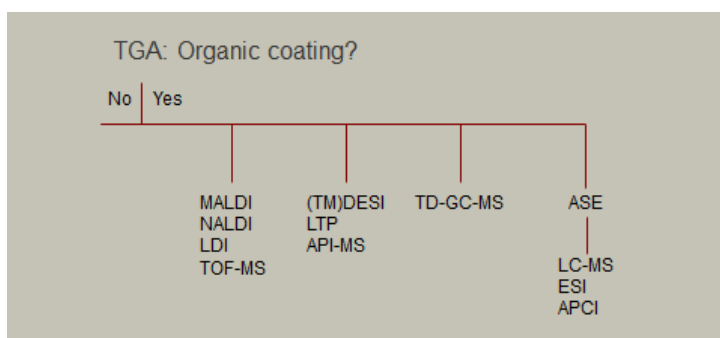


*Figure 0-3 shows a decision tree to help determination of the organic coatings and functionalization*

***ASE (Accelerated Solvent Extraction) or PLE (Pressurized liquid extraction)*** is a fast automatic system for extracting of organic compounds from solid and powder samples. The ASE saves solvent while it accelerates the traditional extraction using high pressure and high temperature (above the boiling point of the solvent). The samples are extracted in cells (1. 5 and 11 ml) under pressure to keep the solvent liquid during the extraction. After heating the extracts are flushed into collecting vials. Optionally, temperature, pressure, extraction volume (mixed solvents) can be varied.

*Sample preparation:*

Cell size has no effect on the extraction time, but strongly influences the amount of the solvent. The cell is filled with solvent during the extraction, therefore, large cells and cells with big dead volume will use more solvent and dilute the sample. Therefore, consider the following: Choose the smallest cell size, which may contain enough sample material to provide a good extraction results.

Remember to clean the cells, sand and filters before use. Place a clean filter on the bottom of the cell and weigh the samples into the cells (about 100 to 500 mg) and fill with sand (Ottawa sand) to reduce the amount of solvent during the extraction. To know the exact volume of the extract it is necessary to weigh the collection vials before and after the extraction.

*Standard parameters:* 2000 psi and 200 °C heated for 10 minute with methanol as solvent in 5 ml cells.

*Materials:* Ottawa sand (Fisher), Methanol 99.9% (Fluka Chromasolv)

Different organic solvents can be used for extraction and therefore it is very important to read the MSDS and Workplace Instruction before starting the extraction.

## TD-GC-MS (analytical thermal desorption (TD) used with gas chromatography (GC) and mass spectrometry (MS) in one systems)

TD is used to detect trace levels of volatile and semi-volatile organic compounds in a wide variety of samples, as for examples environmental pollutants, emissions from materials, food analysis, flavors and dust. The GC in this system is used to separate the component before they entered the MS. If the MS is running in the full scan mode there will typical be monitored a broad range of fragments from 50 to 400 m/z. The most common ionization form is electron ionization (EI). The molecules enter the source where the molecules are bombarded with free electrons emitted from a filament. The most common source is a quadruple or ion trap and the fragments are monitored by a multiplier.

With a TD-GC-MS system there will be a lot of possibilities to vary the parameters as cold-trap, desorption temperature and time, column type, oven temperature, types of ionization, scan modes etc.

The samples can be added into a desorption tube containing a small plug of glass wool and direct desorbed in the TD or this tube can be desorbed in a heated block and transferred the volatile components to an absorbent tube containing e.g. Tenax TA which can then be analyzed with TD-GC-MS. Also a solvent extract from the ASE can be injected into a tube containing Tenax TA (from 5 to 50µl) and subsequently be desorbed in the TD and analyzed with GC-MS.

For quantification a 6 point calibration curve containing the component must be prepared. The components are diluted in methanol and injected on a Tenax TA tube and purged with 60 ml/min nitrogen for 3 min. to evaporate the methanol. These standards are analyzed like the samples.

*Standard parameters:*

*TD:* The absorbent tube was desorbed at 275 °C in 20 min (oven) and the second desorption (cold trap) flash heated from -20 to 300 °C and hold for 1.5 minute. Split 1:10 and the temperature on the valve and transfer line 250°C. Pressure about 16 psi corresponding to 1.3 ml/min trough the column with Helium as the mobile phase (carrier gas).

*GC:* The GC is equipped with a 60 m capillary column with a diameter of 0.32 mm and stationary phase containing 5 % phenyl poly dimethylsiloxane. The initial GC oven temperature of 40ºC was held for 4.0 min, followed by a ramp of 4ºC/min to 120°C and a ramp of 8°C to a final temperature of 250 ºC hold for 4 min.

*MS:* EI (electron ionization) in positive mode. Scan from 50 to 500 m/z. CI (chemical ionization) with methane or ammonia could be a god choice, because the softer ionization can give some information about the molecular ion. CI can be run in both negative and positive mode.

*Materials:* Sampling tubes is made of stainless steel (Perkin Elmer) containing 220 mg 60-80 mesh Tenax TA. All compounds used for standards must be of analytical grade.

# On-column GC-MS

A variation of the above method is direct injection on the column with an auto sampler using liquid samples like the extracts from the PLE. The samples are injected directly into the column by a syringe and swept onto the column.

*Samples preparations:* Liquid samples in a solvent from for example from PLE extraction. The choice of solvent should be considered.

*Standard parameters:*

Temperature program for the oven is as in the above GC-method. The injection volume from the autosampler varies from 0.5 to 5µl samples. The flow is 1 ml/min. helium through the column and the injector temperature at 50°C is hold for 2 min. and then flash heated to 250°C by a ramp of 50°C/min.

*MS:* EI (electron ionization) positive mode. Scan from 50 to 500 m/z.

*Materials:* All compounds used for standards and solvents must be of analytical grade.

# MALDI (Matrix Assisted Laser Desorption/Ionization)

MALDI is a soft ionization technique used for analyzing large molecules. A nitrogen laser beam (337 nm) is iozing the sample in the matrix.. The matrix absorbs the laser energy and it is thought that primarily the matrix is ionized by this event. The matrix is a chemical that easily absorbs the laser energy and a wide range of different chemicals are used for this purpose. The ionized matrix transfer the charges to the sample and the ions will be accelerated in an electro-static field. The mass will be measured in the flight tube in high vacuum by a very precise measurement of the time they are flying (mass analysis of ions with the time-of-flight mass spectrometer).

*Sample preparation:* There are different kinds of sample preparations for MALDI. The easiest preparation is the dried droplet method, where the sample is mixed with a pure solvent e.g. MeOH with or without matrix and applied (0.5 µl) onto a target and dried at room temperature. The target can also consist of different material such as stainless steel or NALDI (nanostructured laser desorption ionization targets) where the surface is covered with a deposited layer of inorganic nanostructures.

*Standard parameters:* Dried drop on stainless steel target suspended in MeOH. Laser beam at 60% and mass range from 200 to 4000 m/z in positive mode. For a better ionization NaCl can be added to the sample.

Materials: Solvents must be of MS grade and standards of analytical grade.

## *Q-TOF (*Quadruple Time of Flight mass spectrometer*)*

The Bruker microTOF-Q mass spectrometer is an ESI Hybrid Quadruple Time of Flight mass spectrometer equipped with a LC-system (liquid chromatography) from Agilent 1200 series. There are different kinds of sources, but the most common is the ESI (electrospray ionization) which generates ion under atmospheric pressure. The formed ions are transferred by an electrical field into the capillary tube and the first stage of the vacuum system. The Q-TOF uses several types of ion guides from the capillary tube to the analyzer passing several vacuum stages. In the TOF part the ions will be pushed into the flight tube by the accelerator unit. The ions fly through the flight tube with different speed depending on their mass until they hit the detector and the time of the flight will be measured exactly. The squared flight time is directly proportional to the mass of the inons. The LC-system is used for separating the component in the samples before they enter the Q-TOFIf the ESI does not work APCI (Atmospheric Pressure Chemical Ionization) could be tried.

*Sample preparation:* Sample preparation depends on the matrix and the sample, but often some cleanup had to be done. Extracts from PLE in a solvent like MeOH can be centrifuges (20000G in 30 min.) to separate out residual particles and the supernatant injected into the LC-system or directly into the ESI on the Q-TOF. If the samples contain very small particles it will be necessary to filter the sample before analysis. SPE (solid phase extraction) can be necessary if the sample for example contains salts.

*Sample analysis:* The chromatographic separation and analysis of the clean extracts were done by using reversed-phase chromatography with a C18 Agilent Zorbax C18 column (4.6 x 12.5 mm particle size 3.5µm) at room temperature with a flow rate of 0.3 ml/min. There are two types of separations on the LC-system, the isocratic or the gradient procedure. It can be a good idea to start with the isocratic run in which the mobile phase does not change during the run and then slowly changing to a gradient run. The mobile phase normally consist of two solvents; solvent **A** is generally HPLC grade water with 0.1% acid and solvent **B** is generally an HPLC grade organic solvent such as acetonitrile or methanol with 0.1% acid. The acid is used to improve the chromatographic peak shape and to provide a source of protons in reverse phase LC/MS. Analytes that are basic in character are generally analyzed in positive ion mode with ESI source. The ionization parameters of the ESI source could be the following: nebulizer gas 1 bar, dry gas 4L/min temperature 190°C. The mass range of the detector is usually set to 50 to 3000 m/z. However, detection of masses up to 20,000 m/z may be achievable.

*Materials:* Solvents must be MS-grade and standards analytical grade

## Additional methods

Additional methods are under development for the SOP. These include DESI, LTP, LDI, and API-MS.

Co-funded by
the Health Programme
of the European Union

## Comments on use and applicability

Due to the high variety of potential organic coatings and the specificity of organic chemical analysis, specific SOPs must be developed for quantification of each organic compound identified in the powder sample.

# SOP for Thermogravimetric Analysis (TGA)

**Renie Birkedal (NRCWE) based on NIST Recommended Practice Guide, Special Publication 960-19**

## General description

TGA is short for thermograviometric analysis. The principle is measuring sample weight as a function of temperature in a given atmosphere at a given heating rate.

TGA is measured according to information wanted and material investigated.

If information about evaporation is wanted heating in $N_2$ is recommended. If information about organic content is wanted heating in $O_2$ or air is recommended, as this will insure combustion of all organic material. In order to make sure e.g. all organic material is decomposed, it is recommended to run to 1000 C.

## Materials and Chemicals:

Powder (may be conditioned in a specific atmosphere and humidity conditions)
Laboratory weigh (scale)
Apparatus for thermogravimetric analysis

## Procedure

### Sample preparation:

- Weigh container.
- Fill container with material. Do not stamp it, as this may affect the evaporation/decomposition temperature.
- Weigh container and material.

For inorganic powder materials a minimum of 10 mg should be used – if possible more. These samples are usually quite homogeneous and this is usually a representative fraction of the sample.

CNT samples are somewhat different. They are in many cases bundles, and these bundles may be different. At the same time these compounds often have a low density, and it is therefore difficult to measure a representative fraction in one or two measurements. The solution is many measurements and comparison of the data.

### Selection of heating rate.

For inorganic materials only a minor fraction is expected to decompose, and a heating rate of 10 C/min is recommended. It is not assumed that there will be large weight losses for these materials,

so this heating rate ensures a fast measurement and most likely still well defined weight losses. If the weight losses are not well defined a slower heating rate can be chosen.

The NIST Recommended Practice Guide, Special Publication 960-19, Measurement Issues in Single Wall Carbon Nanotubes, recommendes a heating rate of 5 C/min. This is chosen as a compromise between time and avoiding too much spontaneous combustion. For some carbon nanotubes 5 C/min is not slow enough to avoid spontaneous combustion. There is no spontaneous combustion with a heating rate of 2.5 C/min. The measurement time is very long, app 7 hours per measurement, but this is still recommended. In order to minimize measuring time it may be an option only to heat to 900 C or even lower.

## Data treatment:

Compare TGA curve and curve for first derivative to find steps of weight loss. It is recommended to obtain several measurements to calculate the mean and standard deviation of the weight loss and the evaporation/decomposition temperatures. (the last is most easily found from the curve of the first derivative). The test of multiple samples also enables evaluation of sample homogeneity.

## ● Contact ●

**Website:**
**www.nanogenotox.eu**

**E-mail:**
nanogenotox@anses.fr

**Coordinator: French Agency for Food, Environmental and Occupational Health & Safety (ANSES)**

27-31, avenue du Général Leclerc
94701 Maisons-Alfort Cedex
France

## Partners

| | | |
|---|---|---|
| French Agency for Food, Environmental and Occupational Health Safety (France) | ANSES | |
| Federal Institute of Risk Assessment (Germany) | BfR | |
| French Atomic Energy Commission (France) | CEA | |
| Institute of Mineralogy and Crystallography (Bulgaria) | IMC-BAS | |
| Veterinary and Agrochemical Research Centre (Belgium) | CODA-CERVA | |
| Finnish Institute of Occupational Health (Finland) | FIOH | |
| Roumen Tsanev Institute of Molecular Biology Academy of Sciences (Bulgaria) | IMB-BAS | |
| Institut national de recherche et de sécurité (France) | INRS | |
| National Health Institute Doutor Ricardo Jorge (Portugal) | INSA | |
| Scientific Institute of Public Health (Belgium) | IPH | |
| Institut Pasteur of Lille (France) | IPL | |
| Istituto superiore di sanità (Italy) | ISS | |
| The Nofer institute of Occupational Medicine (Poland) | NIOM | |
| National Research Centre for the Working Environment (Denmark) | NRCWE | |
| National Institute for Public Health and the Environment (The Netherlands) | RIVM | |
| Universitat Autònoma de Barcelona (Spain) | UAB | |

Co-funded by
the Health Programme
of the European Union

**Grant Agreement n° 2009 21 01**